International Journal of Steel Structures 18(1): 225-253 (2018)
DOI 10.1007/s13296-018-0318-1
ISSN 1598-2351 (Print)
ISSN 2093-6311 (Online)

International Journal of
STEEL
STRUCTURES
www.springer.com/journal/13296

Seismic Design of Coupled Shear Wall Building Linked by Hysteretic Dampers using Energy Based Seismic Design

Bahador Bagheri and Sang-Hoon Oh*

Department of Architectural Engineering, Pusan National University, South Korea

Abstract

In coupled shear wall systems, the excessive shear forces are induced in the coupling beams. As a result, in such systems, the coupling beam and the joint of wall-coupling may yield first. The critical concern about the coupling beam is ductility demand. In order to have such ductility, the coupling beams are required to be properly detailed with significantly complicated reinforcement arrangement and insignificant strength degradation during ground motion. To solve these problems and to increase energy dissipating capacities, this study presents an investigation of the seismic behavior of coupled shear wall-frame system, in which energy dissipation devices are located at the middle portion of the linked beam. The proposed method, which is based on the energy equilibrium method, offers an important design method by the result of increasing energy dissipation capacity and reducing damage to the structure. The design procedure was prescribed and discussed in details. Nonlinear dynamic analysis indicates that, with a proper set of damping parameters, the wall's dynamic responses can be well controlled. Thereafter, an optimized formula is proposed to calculate the distribution of the yield shear force coefficients of energy dissipation devices. Thereby, distributing equal damages through different heights of a building as well as considering the permissible damage at the wall's base. Finally, numerical examples demonstrate the applicability of the proposed methods.

Keywords: Coupled shear wall, damper device, energy based design, optimum deformation ratio, Optimum distribution of yield shear force coefficients of dampers, cumulative plastic deformation ratio

1. Introduction

Concrete structural walls are usually used as the main lateral force resisting system for both medium and high-rise buildings. Due to their high stiffness and strength compared to the mainframe, they absorb considerable lateral forces when the structure is subjected to an earthquake. Architects mostly place these walls near the center of the building around the elevator, and often require that the walls have openings for either doors or windows. The result of having opening at every story level is a reduced lateral stiffness as the structural wall acts more similar to independent walls than a single system. The walls on either side of the opening are thus coupled together by beams. Such a system is called a coupled shear wall.

The structural behavior of reinforced concrete coupled shear wall structures is greatly influenced by the behavior of their coupling beams. Flexure and shear are the two main modes of failure of the reinforced concrete coupling beams (Subedi, 1991). Coupled core wall offers an efficient lateral load resisting system. Performance of a coupled wall system depends primarily on ensuring that the coupling beam provides adequate stiffness and strength (Harries *et al*., 2006).

Coupling beams with low-span depth ratios become shear-critical members which are expected to suffer brittle failure. Special reinforcement details are generally required to avoid the undesirable brittle failure of such coupling beams. As a result of damaging of coupling beams and losing their ability to resist shear forces, the structural deformation may increase significantly due to the reduced system stiffness and the walls will no longer be coupled. To prevent the development of a sliding shear failure and to increase the ductility of coupling beams and energy dissipation capacity, it has been shown (Priestley and Paulay, 1992; Paulay and Binney, 1974; Paulay and Santhakumar, 1976) that for the span to depth ratios of less than two, the combination of diagonal reinforcement with closely spaced transverse reinforcement is required in moderate to highly stressed beams. However, the ACI Building Code (ACI 318-08) proposed the reinforced detailing to ensure stable behavior of coupled beam, which is based on Paulay and Binney's work (1974), is difficult to

Received April 9, 2017; accepted July 13, 2017;
published online March 31, 2018

*Corresponding author
Tel: +82-51-510-7608, Fax: +82-51-514-2230
E-mail: osh@pusan.ac.kr

construct and often fails to maintain the integrity of the full concrete section through large displacement reversals. For simplifying the construction of coupling beam, the ACI building code has recently allowed the use of transverse reinforcement confining the entire coupling beam, as opposed to only the diagonal reinforcement cages. These details have been shown to be effective by Naish *et al.* (2009). Although these details are simpler, these are still hard to construct. Other coupling beam design alternatives have been proposed and investigated (Harries, Gong and Shahrooz, 2000), including various reinforced concrete, steel, and hybrid steel-concrete coupling beam and posttensioned hybrid coupled wall designs (Kurama and Shen, 2004).

There are various methods that have been suggested in order to solve the problem regarding complicated reinforcement details of coupling beam and verified analytically and experimentally (Chung *et al.,* 2009; Kim *et al.,* 2012; Oh *et al.,* 2012) and confining the concrete at the base (I.D.Lefas *et al.,* 1990; Vecchio, 1992) and using the high strength concrete (Parra-Montesinos *et al.,* 2005; Lequesne Rémy *et al*., 2011).

In addition, there have been many researches conducted on the use of damping devices for dissipating seismic energy. These devices can be located within the structure to reduce the demand on the structural elements to absorb energy, and thus, they are designed to protect the building from excessive damage. Madsen *et al.* (2003) used the finite element time history analysis to evaluate the effect of allocating dampers in wall structures. It has been evaluated two approaches; the first approach indicated the dampers parallel to the coupling beams that showed little efficiency due to the presence of the coupling beam, whereas the second approach indicated dampers within openings in the lower stories of the shear walls which was found to be efficient due to allocating the dampers at cut-out sections of the shear wall at lower stories. Sullivan and Lago (2010) highlighted the efficiency of the dampers in reducing important responses in relatively stiff structure. Priestley *et al.* (2007) have shown means for applying their direct displacement based design approach to coupled shear wall systems and suggested to further utilize them by using added dampers of various types.

The objective of this study is to enhance the features of the coupling beams by installing energy dissipation devices with the permissible inelastic deformation demand on the wall piers. This objective is achieved by designing the coupling beam such that most of the inelastic damage would be concentrated in the middle portion of the beam where a damping device would be located. Since in this system, the energy concentrates on the damper devices, means prior action for resisting the lateral force, most of the energy dissipates by this device and would let the wall to reach its capacity demand; thus, important insight on the effect of damper devices in those systems is gained. In order for wall, taking action into permissible inelastic deformation, the characteristics of walls and damper devices such as stiffness, strength and deformation should be well designed. Thus, the optimum yield deformation ratio of the different story buildings is proposed. As a result of implementing the optimum energy dissipation devices, the seismic response of the system such as story drift and the costs associated with upgrading existing buildings will be substantially reduced. The purpose is the development of such systems that will permit a designer to enter certain desired criteria which are based on the energy equilibrium method and to contribute to the understanding of the total behavior of the coupled shear wall building linked by damper devices. Finally, the optimized calculation formula for the distribution of yield shear force coefficients of dampers proposed based on the dynamic analysis results in order to distribute equal damage in the dampers through a different height of buildings. The effect of absorbing energy by dampers is incorporated in the calculation of design vertical shear loads. Every damper is regarded to attain its fully plastic level under the input ground motions.

2. Energy Based Design Background

The equation of motion of an inelastic SDOF system subjected to unidirectional horizontal ground motion can be expressed as follows:

$$M\ddot{y} + C\dot{y} + F(y) = F_e \tag{1}$$

where M is the mass, $C\dot{y}$ is the damping force, $F(y)$ is the restoring force, F_e is the seismic force ($= -M\ddot{z}_0$), z_0 is the horizontal ground motion, y, $\dot{y}$ and $\ddot{y}$ are the relative displacement, first and second derivate with respect to time respectively. Multiplied by $dy = \dot{y}dt$ on both side and integrated over the entire duration of the earthquake, it's reduced to:

$$M\int_{.0}^{t_0} \ddot{y}\dot{y}dt + C\int_{.0}^{t_0} \dot{y}^2 dt + \int_{.0}^{t_0} F(y)\dot{y}dt = \int_{.0}^{t_0} F_e\dot{y}dt \tag{2}$$

Therefore the energy balanced equation becomes:

$$W_s + W_k + W_h = E \tag{3}$$

where W_s is the strain energy which consist of the elastic strain energy W_{es} and the cumulative plastic strain energy W_{ps}, W_k is the kinetic energy, W_h is the energy consumed by damping mechanism and E is the input energy which can be expressed in the form of an equivalent velocity V_E ($= \sqrt{2E/M}$). The kinetic energy and the elastic strain energy constitute the elastic vibrational energy ($0 \le W_e \le (Q_y\delta_y/2)$). Since W_k+W_{es} is the elastic vibrational energy, the Eq. (3) can be expressed as:

$$W_e + W_{ps} = E - W_h \tag{4}$$

Denoting W_e+W_{ps} by E_D, and defining E_D as the energy input attributable to the damage (Housner, 1956), the Eq.

(4) can be rewritten as:

$$W_e + W_{ps} = \frac{MV_D^2}{2} \tag{5}$$

However the above equations imply on inelastic single-degree-of-freedom. In order to express them for a multi-degree-of-freedom (MDOF) subjected to unidirectional horizontal ground motion, the Eq. (1) multiplied by $dy = \dot{y}^T dt$ on both side and integrated over the entire duration of the earthquake, it's reduced to (Benavent-Climent, 2011):

$$M\int_{.0}^{t_0} \ddot{y}\dot{y}^T dt + C\int_{.0}^{t_0} \dot{y}\dot{y}^T dt + \int_{.0}^{t_0} F\dot{y}^T dt = \int_{.0}^{t_0} F_e \dot{y}^T dt \tag{6}$$

where M is the mass matrix, C is the damping matrix and $F(t)$ is the restoring force vector; $\dot{y}(t)$ and $\ddot{y}(t)$ are the velocity and acceleration vectors relative to the ground respectively; F_e is the seismic force ($= -Mr\ddot{z}_g$), r represent the displacement vector $y(t)$ resulting from a unit support displacement.

In the energy-based seismic design approach, design energy input spectra ($V_E - T$) have been proposed in past studies (Akiyama, 1985; Zahrah and Hall, 1985; Benavent-Climent *et al.,* 2002). It has been shown that the total energy induced by the earthquake in MDOF damped inelastic system coincide approximately with that of equivalent elastic SDOF system with 10% damping regardless of changes in distribution of strength, stiffness and of mass at each floor.

2.1. Cumulative plastic deformation ratio

The cumulative plastic deformation ratio of the plastic deformation capacity of the structural component is a dimensionless value which is obtained by dividing the strain energy to yield deformation energy. When the load is removed, the elastic deformation will disappear and the material will return to its original shape. On the other hand, the plastic deformation will not disappear, remaining in the structure, and cumulative up to critical failure condition. Due to the fact that the collapse of a structure usually occurs after the accumulation of some plastic deformation, η most directly indicates the approach of a collapse (Akiyama, 1985). In this case, the strain energy can be used to measure the damage. The definition of the cumulative plastic deformation ratio of each story η is as shown through Eq. (7).

$$\eta_i = \frac{W_{psi}}{Q_{yi}\delta_{yi}} \tag{7}$$

where, W_{psi} is the plastic strain energy, Q_{yi} is the yield shear force and δ_{yi} is the yield deformation on i story.

3. Overview of Shear Wall-frame Interaction Behavior

When a wall-frame structure is loaded laterally, the different free deflected forms of the walls and the frames cause them to interact horizontally through the floor slabs. This study concerned particularly with wall-frame structures that do not twist. The interaction between wall and frame in a wall-frame structure defined by the deflected shapes of a shear wall and a flexural frame subjected to lateral loading. The total behavior of the system is the interaction of the flexural mode of shear wall and the shear mode of frame (Fig. 1A). As a result of interaction, the structure has a flexural profile in the lower part and the shear profile in the upper part. Figure 1B shows the effects of the interaction of wall-frame are given by the curves for deflection, moments, and shears for a typical wall-frame structure (Smith and Coull, 1991). The efficiency of frame systems in dual (wall-frame) tall bending for reducing the horizontal displacements and wall bending moments under lateral load has been long known (Rosmon, 1964; Bertero, 1980). It was revealed that in such systems,

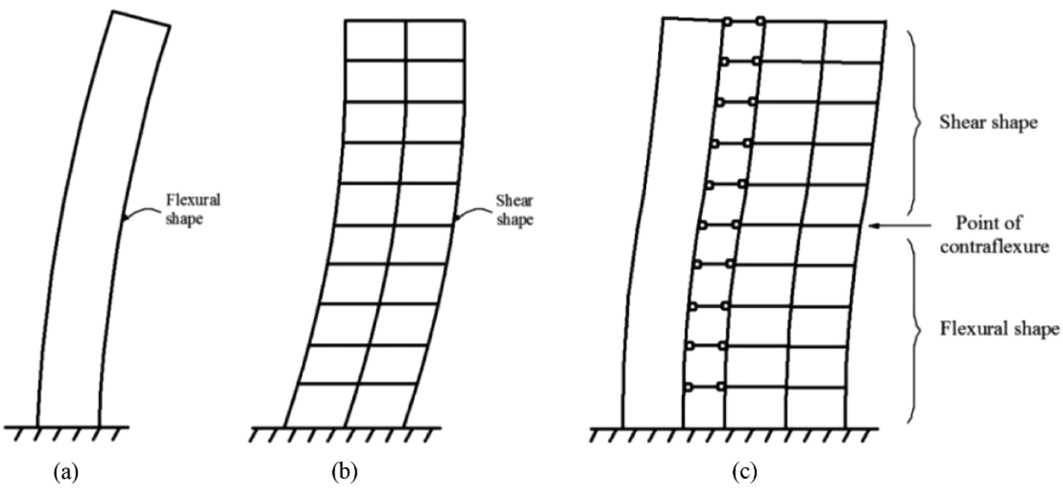

Figure 1A. (a) Flexural behavior of wall (b) Shear behavior of frame (c) Flexural-Shear behavior of wall-frame.

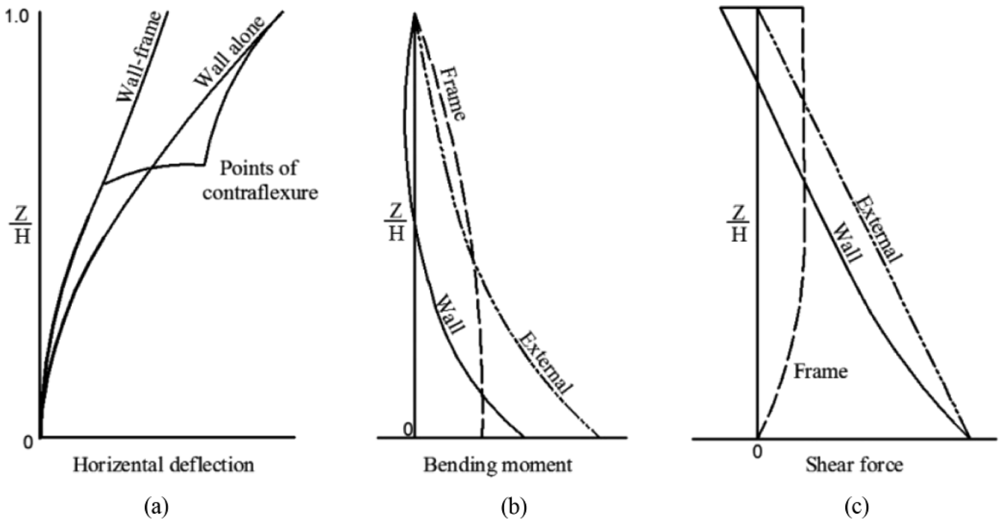

Figure 1B. (a) Typical deflection diagram of laterally loaded wall-frame structure (b) Typical moment diagram for components of wall-frame structure (c) Typical shear diagram for component of wall-frame structure.

shear walls restrain the inter-story drift in the lower stories due to the controlled deformation by bending moment. The flexural frames effectively restrain the inter story drift due to the controlled deformation by story shear, and hence the shear walls at the top. In addition, the flexural frame also leads to a reduction of the bending moment at the base of the walls.

4. Case Study and Analysis Model

For this study, only the coupled core wall of the structure is considered to contribute to the lateral resistance of the structure. It means, only shear wall experience plastic deformation during an earth quake and the frame remain at elastic. The major structures considered are based on 10, 15 and 20 story buildings and for the sake of comparison; the 16, 17, 18 and 19 story buildings will be added in this study. The plan of the structures and the general geometry for the parametric study is shown in Fig. 2. The model considers wall as a line element (Fig. 3) (Column element) located at the wall central line. Bending, shear and axial springs are used to present the wall deformation in the wall plane. The plane section assumption is applied to determine the rotation at the wall base and top sections from the node vertical translations at the wall four corners. The edge columns for modelling

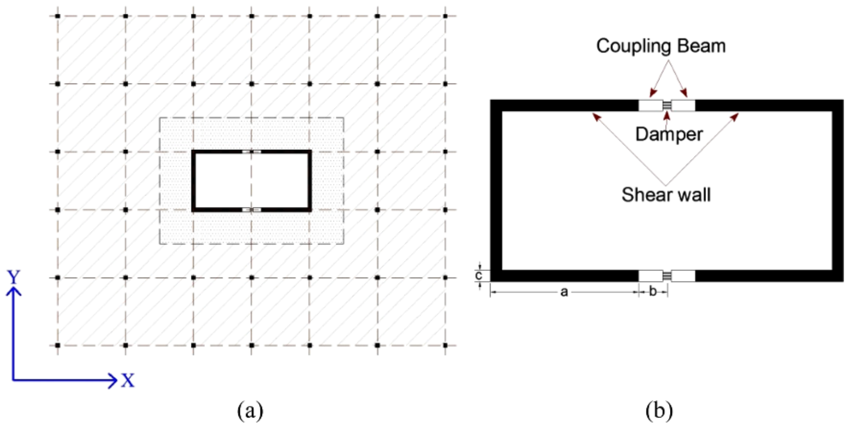

Figure 2. (a) Plan of the structure (b) the geometry of core coupled shear wall.

Table 1. Walls section properties

	a (m)	b (m)	c (m)	EI (kN·m^2) (Flexural stiffness)	AG/(6/5) (kN·m) (Shear stiffness)	AE (kN) (Axial Stiffness, compression)
System 1	4	1	0.45	56660280	14755281	42495210
System 2	5	1	0.45	110664609	18444101.25	53119013

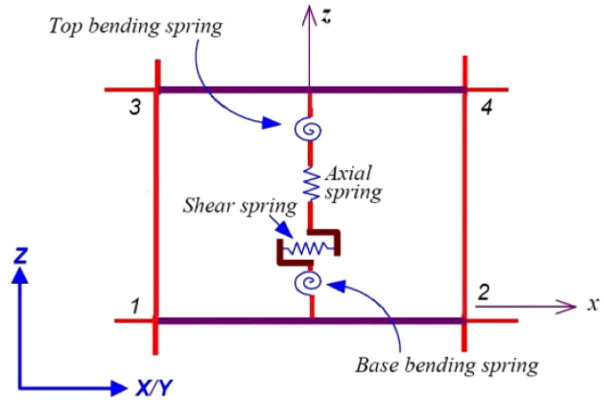

Figure 3. Wall model.

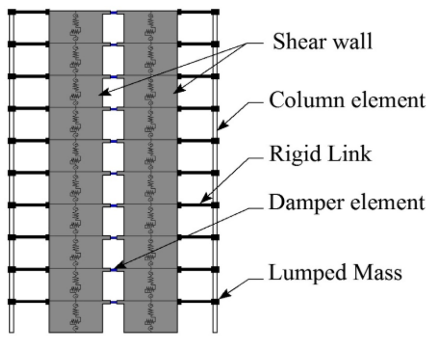

Figure 4. Shear wall-frame structure model.

of the core shear wall are not considered here.

The properties of the geometry of core walls are provided in Table 1. For the initial parametric study, gross section properties were used for the wall piers in order to calculate the flexural, shear and axial stiffness. The walls were modeled with flexural springs on both ends, because the damage is concentrated in the hinge area of both ends of wall members. The effect of different assumptions of effective properties will be discussed later in this paper. The prototype is a reinforced concrete frame with double channel core wall linked by the dampers at the center of the coupling beams. Both wall piers are identical. The walls have a uniform thickness of 450 mm over their entire height. Story heights are also constant at 3000 mm. For evaluation purposes, the coupling beams with infinite stiffness were applied to the model shape in order to facilitate the story specific design. The structure surrounding the core is assumed to be symmetric. Torsion will not be considered in this initial investigation. A lumped mass was placed at each node of the columns and outer side of the shear walls that intersected the floor level (Fig. 4). It is assumed that concrete having a compressive strength of f_c'=21 MPa and a modulus of E =23600 MPa, steel rebar having yield tensile strength of σ_y=350 MPa and a modulus of E =205000 MPa will be used throughout the structure in order for computing the flexural, shear and axial strength of the members. The rebar's placement is not the purpose of this paper.

The columns of the frame are designed to carry only gravity load. Therefore the lateral resistance mechanism of this system is coupled shear wall linked by damper device.

The damage distribution of 10, 15 and 20 story building with variable cross sections of the shear wall, stiffness and strength of the dampers are discussed here. The mass distribution is to be uniform. The stiffness distribution of core shear wall, main frame and damper in each case are to be uniform. The bilinear hysteretic model is used to describe the force-displacement relationship of flexural and shear springs in this design model at each story level. Bilinear hysteretic has been the most widely studied in type of hysteretic nonlinearity and in order to facilitate the

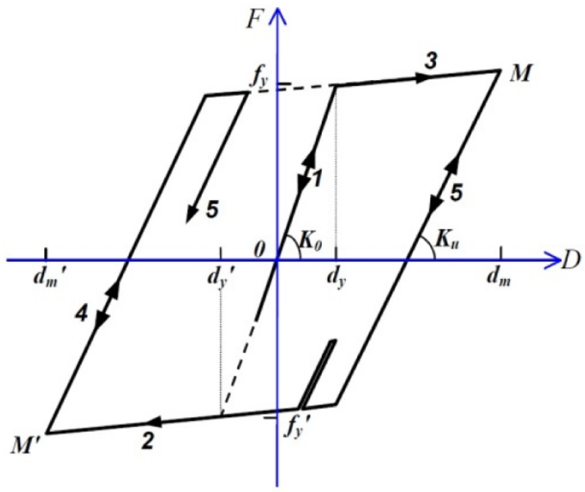

(a) Degrading bilinear model

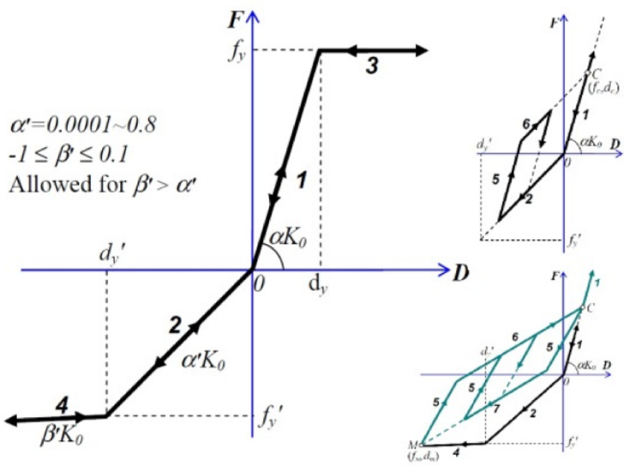

(b) Axial stiffness model

Figure 5. Hysteretic models.

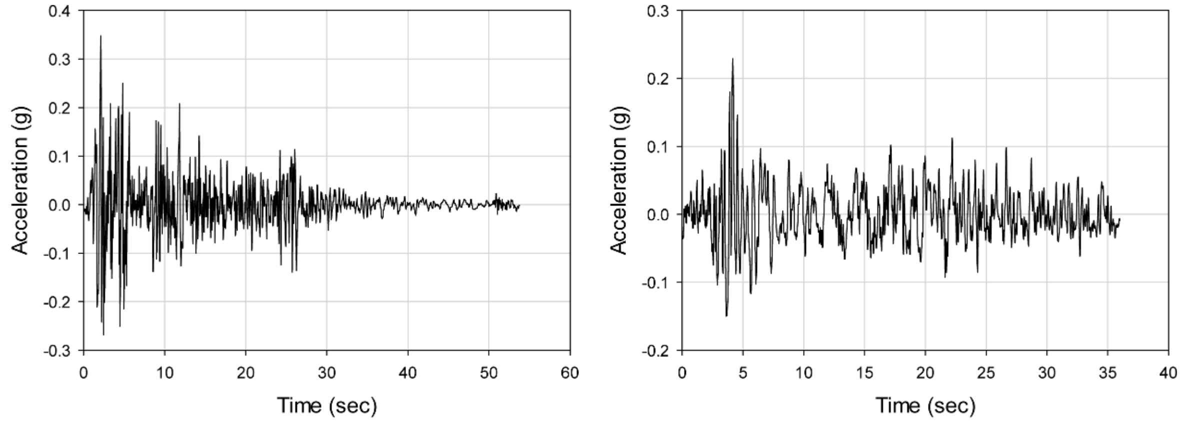

(a) El Centro NS 1940 (b) Hachinohe NS 1968

Figure 6A. Earthquake records.

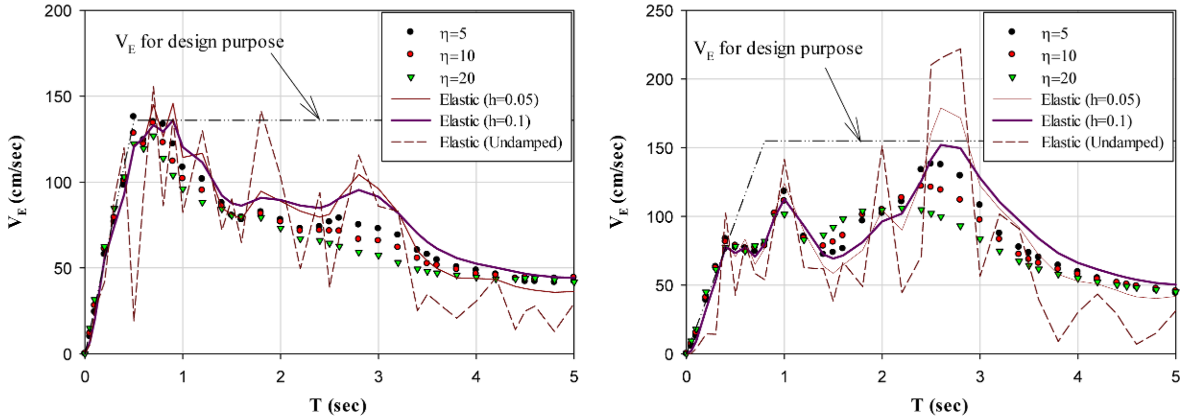

(a) El Centro NS 1940 (b) Hachinohe NS 1968

Figure 6B. Response Energy Spectrums of SDOF system.

identification of the basic design variables and relationships between them. Figure 5(a) illustrates a plot of restoring force versus displacement (or restoring moment versus angle) for the bilinear hysteretic springs. Strain hardening modulus was set to 0.1 and 0.01% of the elastic modulus for the structural members and damper devices respectively. The model for the axial stiffness is intended to present the axial compression and tension stiffness of reinforced concrete materials. It has tension crack and yielding rules, and unloading/reloading rules of load changing between tension and compression Fig. 5(b). The damping system considered as 5%. The ground motions selected are the record of the 1940 El Centro NS earthquake and the record of the 1968 Hachinohe NS earthquake (Fig. 6A). For the seismic design purpose, the energy input for each record is shown in Fig. 6B. The proposed values for each record correspond to an upper bound of energy inputs in the inelastic systems with having different cumulative plastic deformation ratio and elastic system with the damping ratio of 10% (h =0.1). Therefore, it is thought that in order to design a more reliable passive control structure, energy spectrum, rather than acceleration response spectrum, should be used as the design spectrum.

4.1. Coupled shear wall system with damping devices

Figure 7 shows the detail of the placement of damper at the middle portion of the coupling beam. The size of damper determines the width of the vertical slit in the middle of the coupling beam. The shear strength of coupling beams are greater than the maximum damping force of dampers, therefore it can meet the requirement for dissipation the energy. The benefit of using this method is that it prevents the confliction between ductility and strength in the design of the coupling beam.

The schematic of the spring model of damper in coupling beam is shown in Fig. 8. The shear spring can be effective to dissipate energy if the wall dislocate as Fig. 9. The dislocation between slit coupling beams is composed of several component: δ_1, δ_2, δ_3 and δ_4. As it is shown in the geometry of the wall, the coupling beams are connected by dampers rather than slit entirely, therefore total dislocation should be zero, i.e. $\Sigma\delta_i = \delta_1 + \delta_2 + \delta_4 = 0$. δ_2 and δ_3 can be regarded as zero, because most of the energy concentrate at the dampers, therefore the deformation

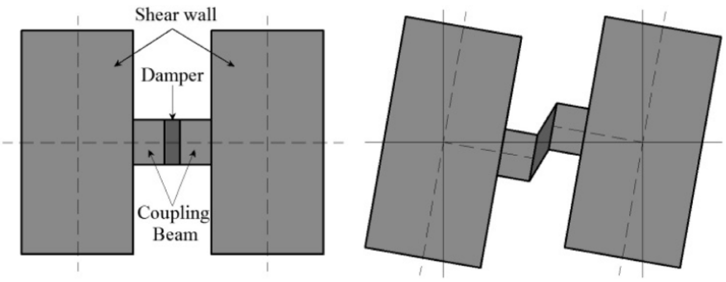

(a) Un-deformed shape (b) Deformed shape

Figure 7. Behavior of coupled shear wall with energy dissipation devices.

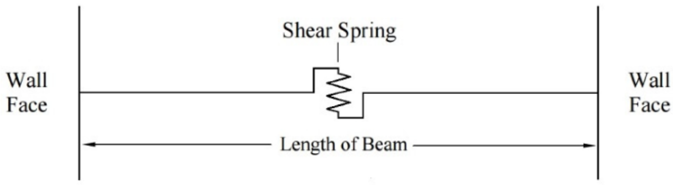

Figure 8. Spring model of damper in coupling beam.

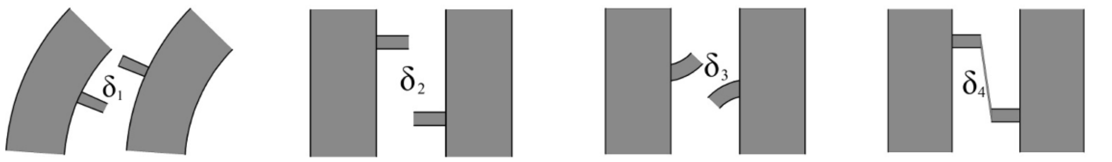

(a) shearing and bending deformation of wall piers (b) Axial deformation of deformation of wall piers (c) shearing and bending coupling beam (d) deformation of damper

Figure 9. Exaggerated vertical dislocations between the wall piers.

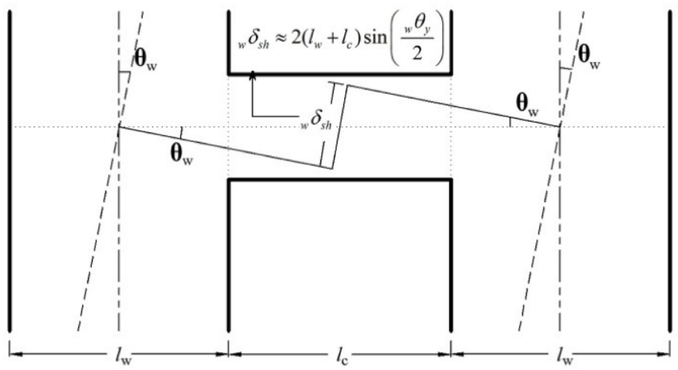

Figure 10. Relationship of displacement between coupling beams and wall piers.

will predominantly concentrate in the dampers, it means $\delta_1 \approx \delta_4$. The damper that installed as a coupling beam system between two walls uses the flexural deformation of the shear wall to undergo large plastic deformation. As shown in Fig. 10, the rotation (θ_w) occurs at the center of the wall when the flexural deformation of two wall piers is induced by the lateral load. Two wall piers are rotated about θ_w by the lateral load, so according to this rotation, the vertical deformations occur in the center beam where the damper located. The deflection of the dampers can be expressed as ${}_D\delta \approx 2(l_w + l_c)\sin(\theta_w / 2)$ while l_c is the span of coupling beam, l_w is the width of wall pier, θ_w is the wall pier's rotate angle.

In this model the stiffness of dampers selected as a ratio of flexural stiffness of the walls, i.e. ${}_D k_T = K \times {}_{fl} k_{w_T}$, where ${}_D k_T$ is the sum of the stiffness of dampers which placed in parallel (${}_D k_T = {}_D k_1 + {}_D k_2 + {}_D k_3 + \ldots + {}_D k_n$), ${}_{fl} k_{w_T}$ is the sum of the flexural stiffness of wall piers which placed in series ($(1/{}_{fl}k_{w_T})=(1/{}_{fl}k_{w_1})+(1/{}_{fl}k_{w_2})+(1/{}_{fl}k_{w_3})+\ldots+(1/{}_{fl}k_{w_n})$) and K is the ratio of stiffness of dampers to the flexural stiffness of walls ($0.05 \le K \le 1$).

The first design parameter that needs to be taken into

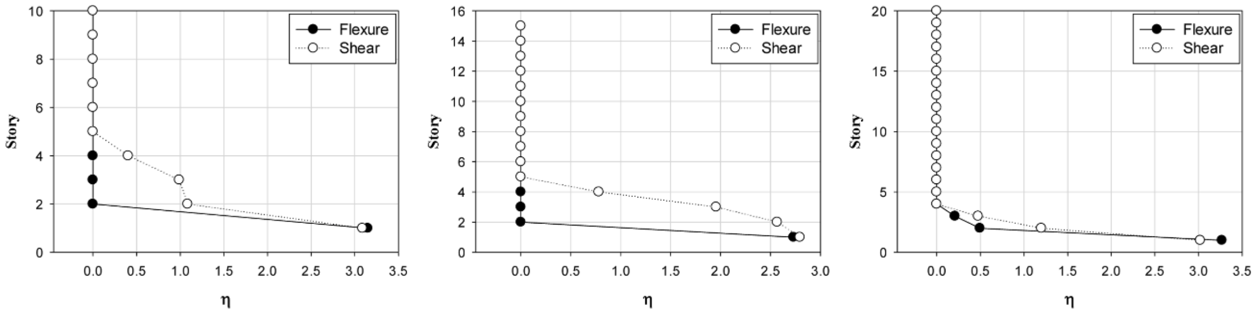

(a) 10 story building (b) 15 story building (c) 20 story building

Figure 11. Cumulative plastic deformations of walls in flexure and shear.

account is the yield displacement of the dampers. They are naturally expected to yield before the shear wall might yield. However, the deformation of dampers is along vertical direction, but structural inter story drift is horizontally. In addition, in order for dampers taking action into plastic deformation, the walls should be checked in flexural behavior. Dampers need to undergo large plastic deformation (larger than δ_y) to dissipate energy. When using the damper device, the yield deformation of the damper is smaller than that of the yield deformation which caused by flexural response of shear wall, so the damper device begins dissipating energy before the shear wall might yield. The required yield displacement of dampers may be specified as Eq. (8).

$$ {}_D\delta_y < 2(l_w + l_c)\sin\left(\frac{{}_w\theta_y}{2}\right) \tag{8} $$

${}_D\delta_y$ is the yield deformation of damper. It can be shown as ratio of total yield strengths of dampers to total stiffness of dampers (${}_DQ_{yT}/{}_Dk_T$). Therefore the Eq. (8) becomes as follow:

$$ \frac{N\cdot{}_DQ_{y1}}{K\cdot{}_{fl}k_{w_T}} < 2(l_w + l_c)\sin\left(\frac{{}_w\theta_y}{2}\right) \tag{9} $$

where, N is the number of stories.

The flexural and shear strengths of each wall are designed based on having η=6 in the first story as the limit state in this study ($\eta = \eta_{fl}+\eta_{sh}$). When using damper device in the coupled shear wall system, the lateral load resisting behavior of the wall group changes to one where structural overturning moments are resisted partially by a shear action in the dampers rather than only by the individual flexural action of the walls.

In order to show the influence of dampers' parameters such as stiffness, yield strength and yield deformation, on the behavior of shear wall in flexure and shear, the shear walls are designed for the specific plastic deformation in shear and flexure at the wall bases. In order to achieve such a plastic deformation, the dampers that link the shear wall considered once as a flexible device with having insignificant stiffness and high strength value for all types of structures. Hence, the input energy dissipates only by shear wall and most of the energy input concentrates in the first story wall piers (Fig. 11). Then, by increasing the stiffness ratio, the walls tend to behave in a different manner. Therefore, the cumulative shear and flexural plastic deformation are changed. However the total behavior of shear walls doesn't depend only on the stiffness of the dampers, it more depends on the strength of the dampers.

5. Investigation on the Behavior of Walls at the Specified Range of Natural Vibration Periods

The prior structures designed at the specific permissible damage at the wall's base when the dampers are flexible. The stiffness of dampers are decided as a ratio of flexural stiffness of wall at the base.

Regarding the parameters of dampers and the influence of wall stiffness and geometrical dimension, two ratios are defined as below:

(1) $Q_{yD}/Q_{yfl,1}$, which is Q_{yD} is the sum of yield strength of dampers in all stories and $Q_{yfl,1}$ is the flexural strength of shear walls at the first story.

(2) ${}_D\delta_y/{}_w\delta_{sh}$, which is ${}_D\delta_y$ is the yield deformation of damper and ${}_w\delta_{sh}$ is the deformation at the middle portion of the beam in the first story induced by flexural behavior of shear walls (${}_w\delta_{sh} = 2(l_w + l_c)\sin({}_w\theta_y/2)$).

In accordance to the energy dissipated by dampers, in the lower stories, the dampers work inefficiently and dissipate less energy compared to the middle and upper portion of the system. As the shear wall intends to deform during an earthquake, the slope of the deformation curve will be increased up to the contraflexure point, means, the dampers experience large deformation at the middle stories regardless of the height of shear walls. At the upper portion of the walls, there will be a reduction of dampers' dissipative efficiency; because the total behavior of the wall-frame system in the upper portion is shear, therefore the slope of the deformation curve descent partly. However, at the high dissipation energy by dampers, the value of the maximum damage at the upper part would be

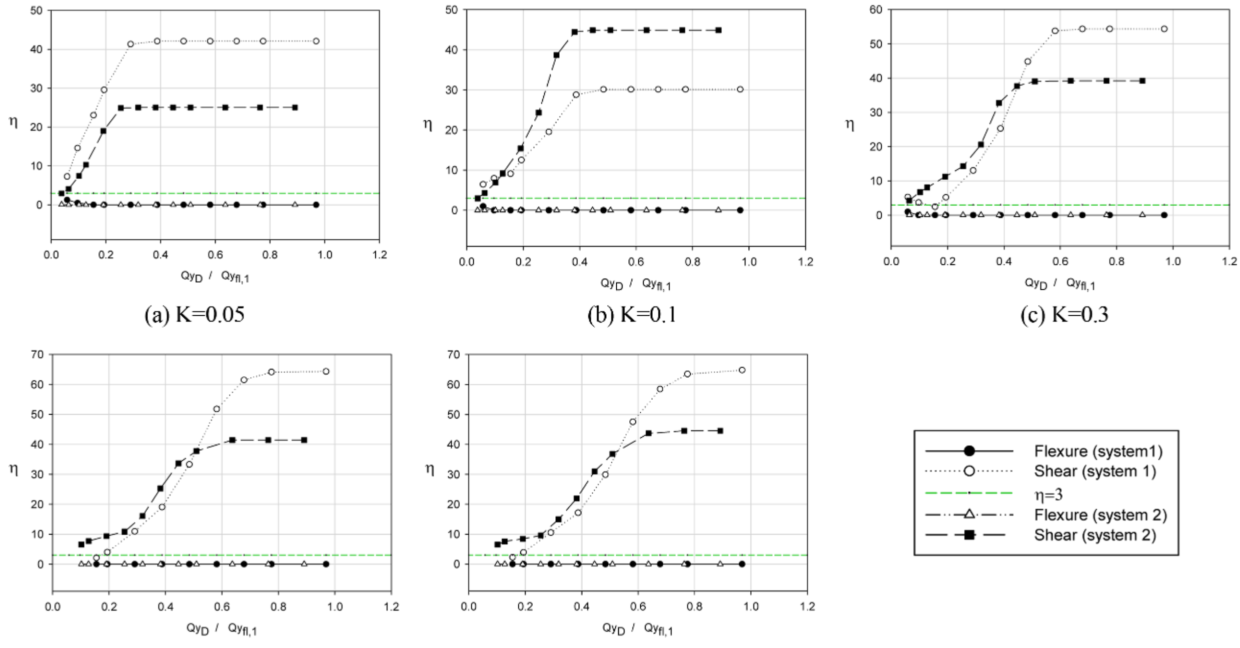

(a) K=0.05 (b) K=0.1 (c) K=0.3

(d) K=0.6 (e) K=1

Figure 12. damage response at 10 story buildings (El Centro NS 1940).

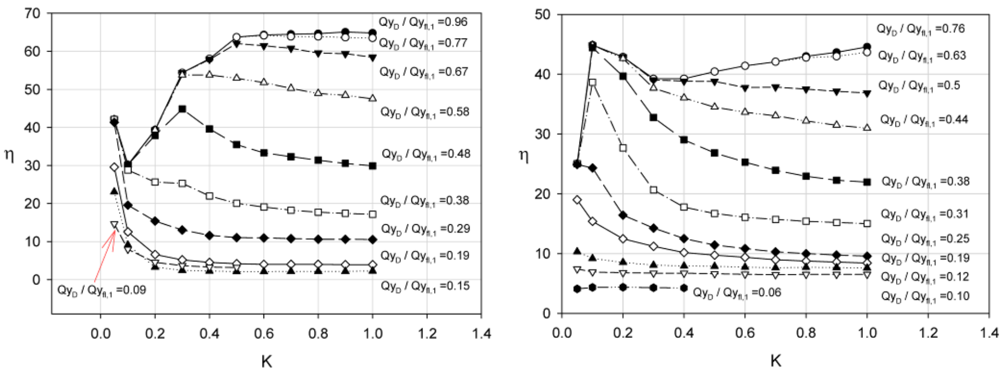

(a) System 1 (b) System 2

Figure 13. Cumulative shear plastic deformations at the base of shear wall (10 story, El Centro NS 1940).

the equal amount of damage at the middle height of the system.

The numerical results of 10, 15 and 20 story of systems one and two which is plotted from Figs. 12-18 for the record of El Centro NS 1940, demonstrate how the damage at wall change with damper characteristics such as stiffness and yielding deformation. Figures 12, 15 and 17 shows the flexural and shear cumulative plastic deformation at wall piers for 10, 15 and 20 story buildings calculated by Eq. (7) respectively, which demonstrate how the wall's responses change with the variety of stiffness and strength of dampers. In each graph, the yield strength ratio change with the constant stiffness ratio.

The natural vibration periods of the systems are as follow: 10 story buildings T_{sys1} =0.6 sec, T_{sys2} =0.56 sec, 15 story buildings T_{sys1} =1.14 sec, T_{sys2} =1.02 sec and 20 story buildings T_{sys1} =1.9 sec, T_{sys2} =1.69 sec.

It is concluded that by increasing the stiffness ratio of wall-frame, although the shear and flexural cumulative plastic deformation of wall piers of both systems are equal at the base, the shear damage will be decreased. It is clear that by increasing the stiffness of the dampers, the flexural cumulative plastic deformation of wall piers at first story will be zero and walls show the shear behavior when K rises. In 10 and 15 story buildings, at the higher yield strength ratio (0.5-1), the amount of shear cumulative plastic deformation at wall piers will be gradually increased and will be constant at the specific range of stiffness ratio (0.5-1 and 0.6-1 for 10 and 15 story buildings respectively). Whereas, at the lower yield ratio (0.09-0.5) the cumulative shear plastic deformation will be decreased (Figs. 12 and 15). Meanwhile, in 20 story buildings, the shear and flexural damage at walls are less by using damper at any range of stiffness and yield strength ratio (Fig. 17).

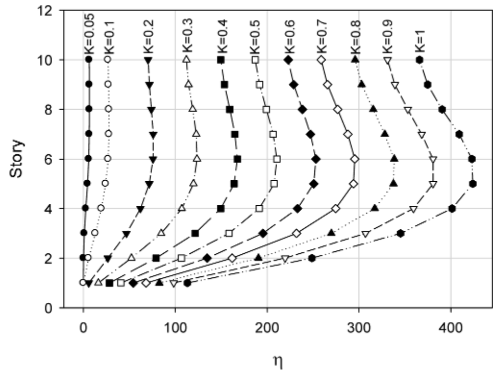

Figure 14. Cumulative shear plastic deformations at dampers (10 story, El Centro NS 1940).

However, the results prove that selecting the dampers with relatively high stiffness will not reduce the damage at walls, but it more depends on the yield strength ratio. Figures 13, 16 and 18 represent how the wall's response change as the stiffness ratio rises with the different yield strength ratio. In the low and high stiffness ratio, at the lower yield strength ratio, the cumulative shear plastic deformation at walls almost identical and most of the input energy was predominantly dissipated by the dampers. Because of using the low yield strength ratio, the shear walls behave in flexural and thus, the damper dissipates more energy. However, it is worth to note that based on the results in Fig. 18, selecting a very low strength ratio would cause more damage at the wall base and must be

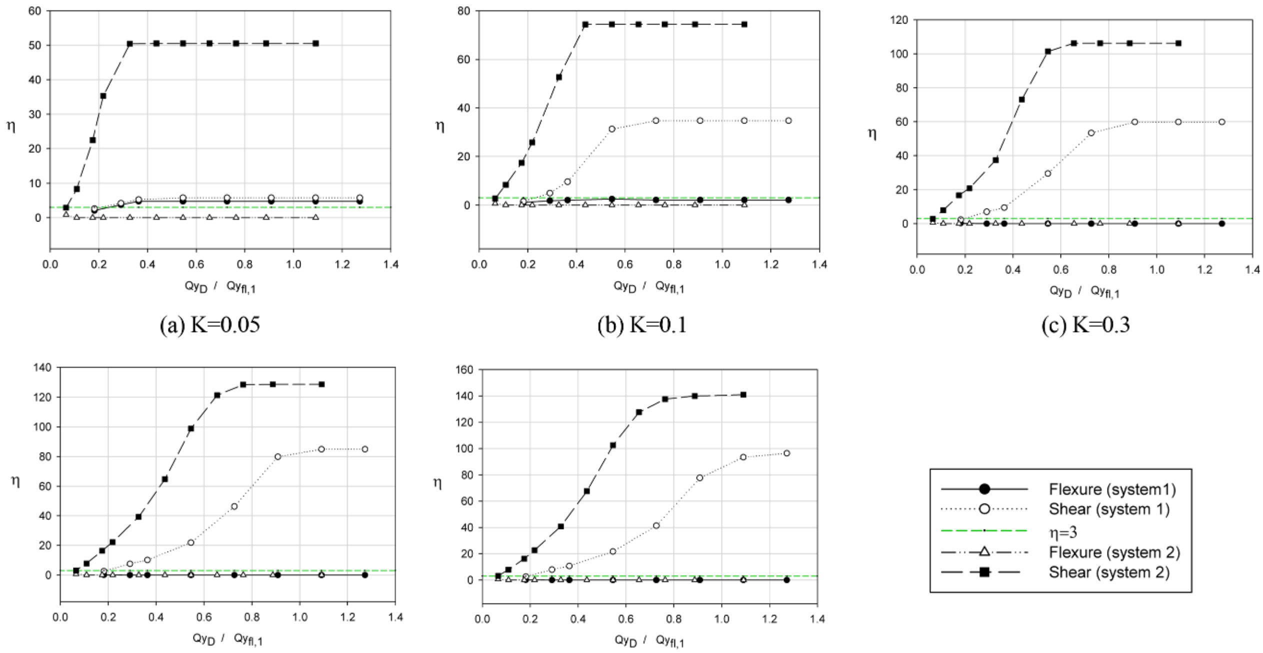

(a) K=0.05 (b) K=0.1 (c) K=0.3

(c) K=0.6 (d) K=1

Figure 15. damage response at 15 story buildings (El Centro NS 1940).

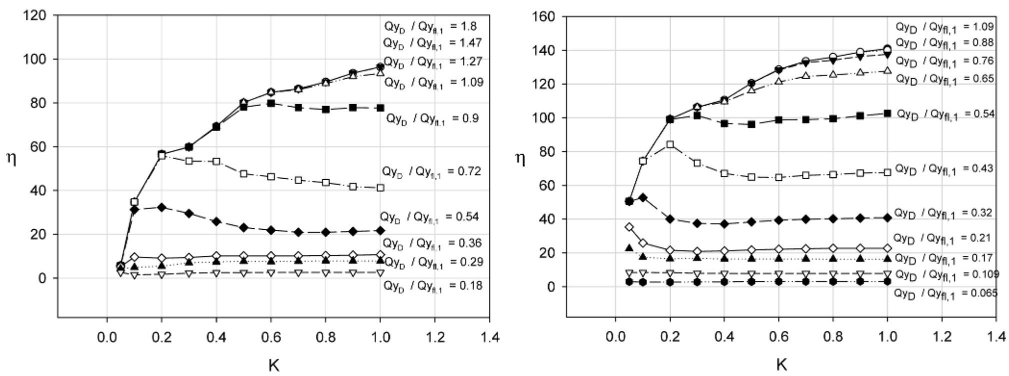

(a) System 1 (b) System 2

Figure 16. Cumulative shear plastic deformations at the base of shear wall (15 story, El Centro NS 1940).

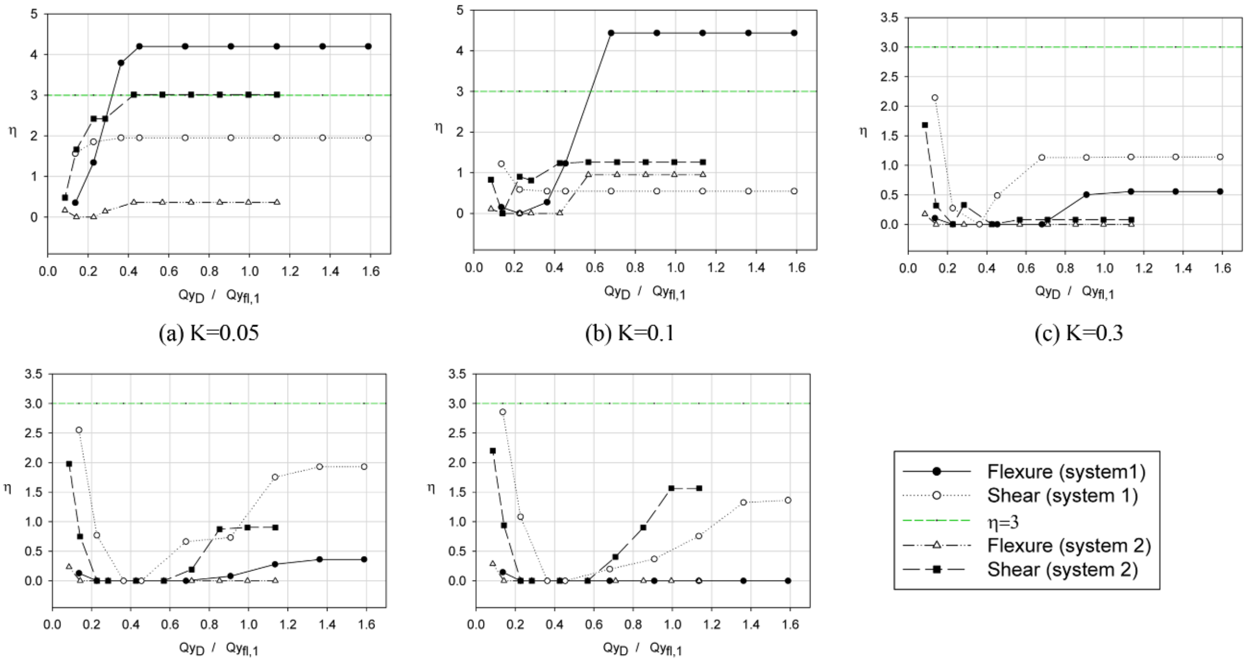

(a) K=0.05 (b) K=0.1 (c) K=0.3

(c) K=0.6 (d) K=1

Figure 17. damage response at 20 story buildings (El Centro NS 1940).

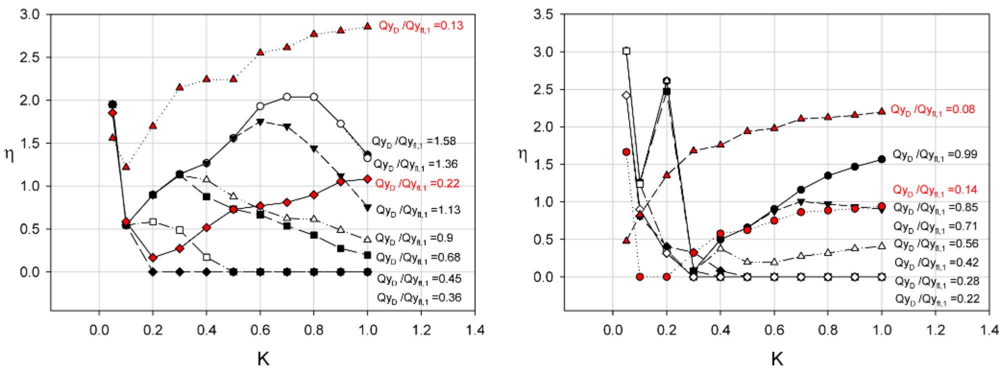

(a) System 1 (b) System 2

Figure 18. Cumulative shear plastic deformations at the base of shear wall (20 story building, El Centro NS 1940).

taken into consideration. In addition, shear damage in the structure with high strength ratio would be increased by increasing the stiffness ratio. The difference of selecting the different stiffness ratio will affect the amount of dissipated energy by dampers. At the lower stiffness ratio (K) the dissipation energy by dampers is less than that of in higher stiffness ratio for the specific yield strength ratio. Figure 14 shows the damage at dampers in different stiffness ratio and the constant yield strength ratio of 0.19 for the system 1 (10 story).

5.1. Damage distribution at dampers

By increasing the yield strength ratio, means increasing the yield strength of dampers, the damage concentrate at the lower part, because of the flexural behavior of a system at the lower part. At the upper part, the deflected shape of the system is shear, thus the walls behave with the different slope from the contraflexure point, and therefore the total damage on the upper part depends on the amount of damage on the lower part. For instance, Fig. 19 shows the damage at dampers when K=0.6 with the different yield strength ratio. Table 2 shows the ratios selected as dampers start dissipating energy. At the high yield strength ratio, dampers dissipate less energy, means less damage, but by decreasing the yield strength ratio, the damage at dampers will be increased and also the damage at upper part will be close to the amount of damage at the contraflexure point.

5.2. Performance of walls at the different deformation ratio

Multiple response curve with different deformation

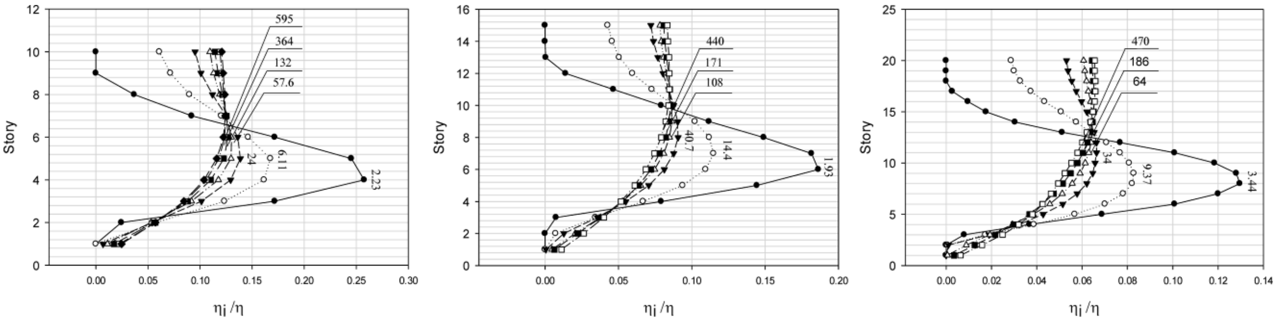

(a) 10 story (b) 15 story (c) 20 story

Figure 19. variation of behavior and damage of dampers (El Centro NS 1940).

Table 2. Strength ratio of dampers to the wall base

No of story	$Qy_D/Q_{yfl,1}$						
10	0.67	0.58	0.48	0.38	0.29	0.19	0.15
15	0.9	0.72	0.54	0.36	0.29	0.18	-
20	0.9	0.68	0.45	0.36	0.22	0.13	-

ratio ($_D\delta_y/_w\delta_{sh}$) for the wall piers and dampers are given in Figs. 20, 22 and 24 for the 10, 15 and 20 story buildings respectively. It is obviously showing that the shear response of wall piers would be better controlled with a lower deformation ratio in a certain range. In Figs. 20(a) and 22(a), the shear responses in the system one, have the similar variation tendency with the system two at the lower specific range of deformation ratio for the El Centro 1940 record. Therefore, only the response of system two is given in the Hachinohe record. Besides, Figs. 20(c), 22(c) and 24(c) represent the relationship between dampers' response and deformation ratio. When the dampers have very small yield deformation ($_D\delta_y$), the dissipation energy is high which reduce the shear response at wall piers in the same range notably. The variety of stiffness causes the difference of dissipated energy at the lower yield deformation ratio. The observation is associated with the fact that the points of the upper bound show the high stiffness selected and reverse the points of lower bound show the low stiffness selected for the energy dissipation devices. However, by selection the optimum range of deformation ratio, the shear strength of wall piers still need to be increased either by adding shear reinforcement or increasing the shear size of the walls. However, increasing the amount of shear strength is different for different height story buildings and natural vibration period; therefore the percentage of increasing depends on the amount of shear damage at the base of wall piers. As it is shown in Figs. 20, 22 and 24, the optimum range for the deformation ratio is selected in order to get less damage at the wall's base. Regarding by selecting the best range for the deformation ratio, the damage at the upper stories of the base would be less as well relatively. In order to obtain the maximum damage in dampers at corresponding optimum range, regarding to the damage at wall base, the Figs. 20(c), 22(c), 24(c), 28(c), 29(c), 30(c), 31(c) and 32(c) demonstrate the relation between deformation ratio and the amount of maximum damage at dampers. It proves that the less deformation ratio, the more dissipated energy achieved. Figures 21 and 23 represent the damage distribution through height at the optimum deformation ratio without amplification factor which only concentrates at lower stories. It is clarified that the maximum shear damage distributions through height at any range of optimum deformation ratio are almost similar.

The results prove that the shear wall behave in shear at high response up to 15 story building (Fig. 25). From 16 to 20 story building, the shear damage on walls would be at the permissible damage rate.

5.3. Flexural strength reduction factor (FSRF) at walls

The general design philosophy of dampers is to ensure that the dampers begin dissipating energy while the wall piers reach its capacity demand. The strength reduction factor is an important key for developing the seismic design theory and improving the reliability of the structures.

In order to allow the applicability of this design approach within the actually widespread seismic design approach (i.e. Nonlinear time history analysis with force reduction factor), it is clear that the insertion of energy dissipation devices into a coupled shear wall system reduces the overall flexural ductility demand. Thus, if the designer decides to account for the ductility capacity of the structural members and the dissipative properties of the added dampers, only one analysis method is actually available: a fully non-linear time-history analysis. With the purpose of extending the use of energy dissipative devices to a wider range of coupled shear wall building structures, the present paper proposes a simple formulation for the flexural strength reduction R_F in the case of coupled shear wall buildings equipped with damper devices to demonstrate the value of reduction in the following sections. The use of such reduction factors in walls with damper devices allows satisfying a criterion of equal safety in the walls equipped with added damper devices.

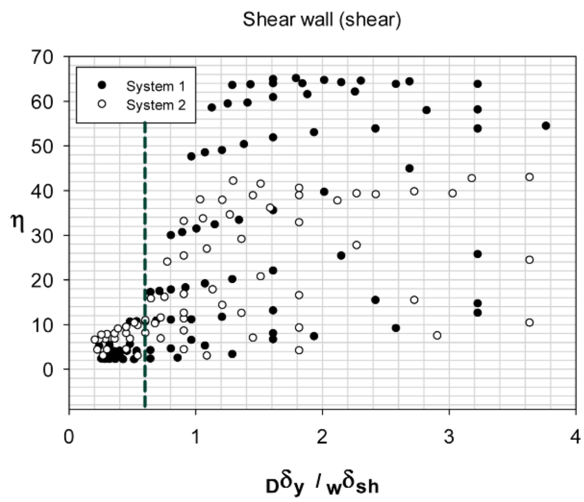

(a) Shear wall at base (shear damage response El Centro NS)

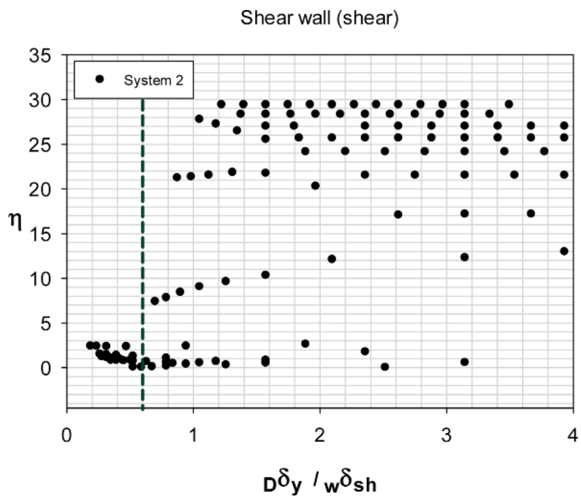

(b) Shear wall at base (shear damage response Hachinohe NS)

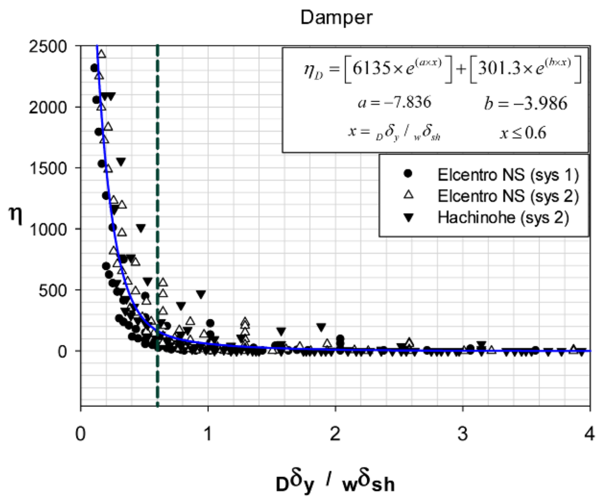

(c) Maximum damage response of dampers

Figure 20. Structural responses due to variation of $_D\delta_y$ (10 Story, T_{sys1} =0.6 sec, T_{sys2} =0.56 sec).

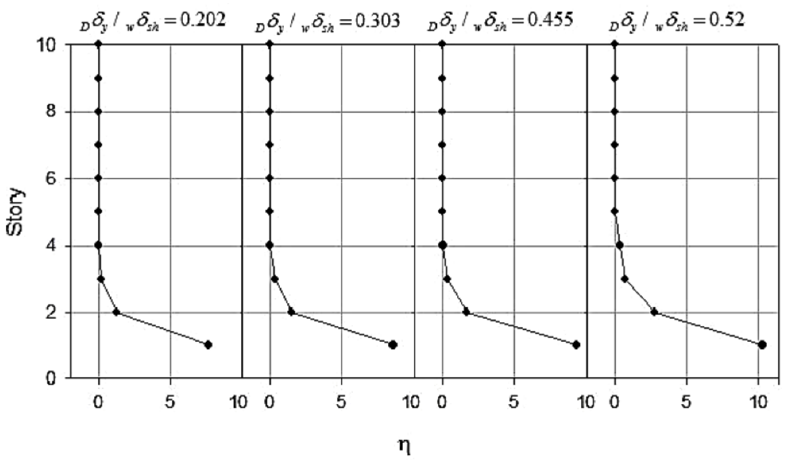

Figure 21. Distribution of cumulative shear plastic deformation of wall piers at different deformation ratio (El Centro NS).

The flexural strength response of the system two computed at the optimum deformation ratio. The huge number of numerical analysis proves that in order to obtain an optimum flexural strength of the wall, the characteristics of damper should be designed based on the optimum deformation ratio for all the cases.

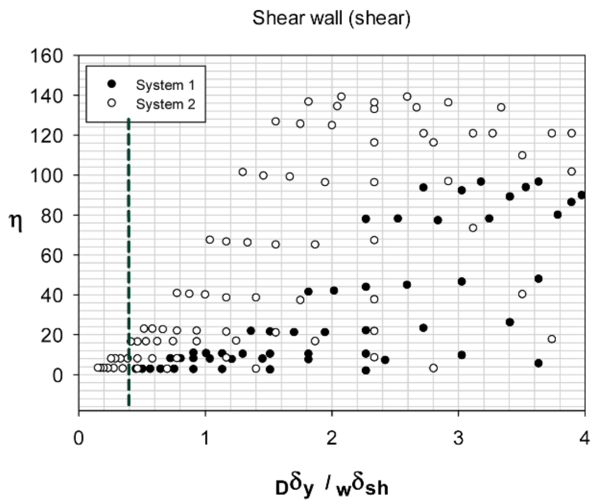

(a) Shear wall at base (shear damage response El Centro NS)

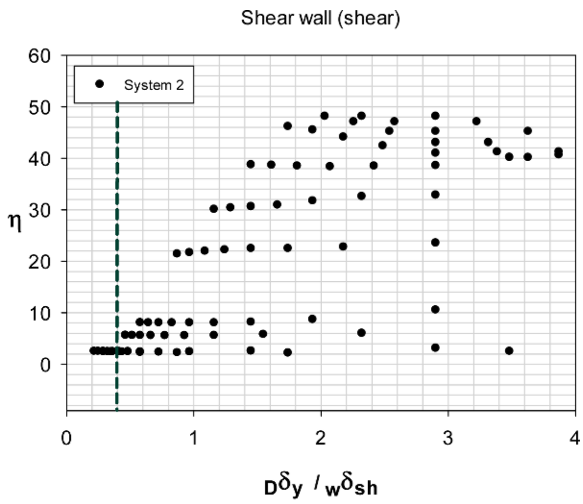

(b) Shear wall at base (shear damage response Hachinohe NS)

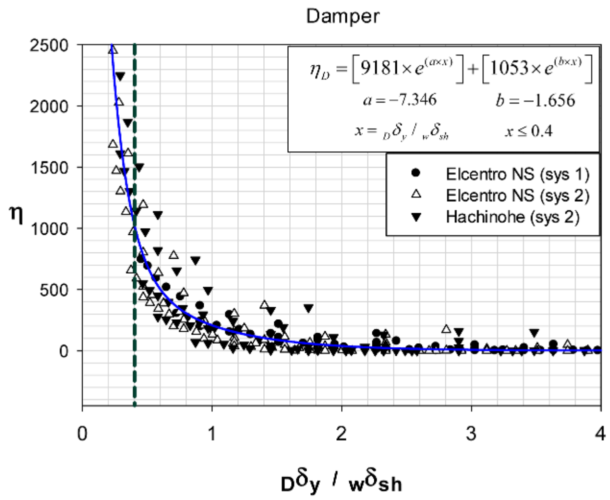

(c) maximum damage response of dampers

Figure 22. Structural responses due to variation of $_D\delta_y$ (15 Story, T_{sys1} =1.14 sec, T_{sys2} =1.02 sec).

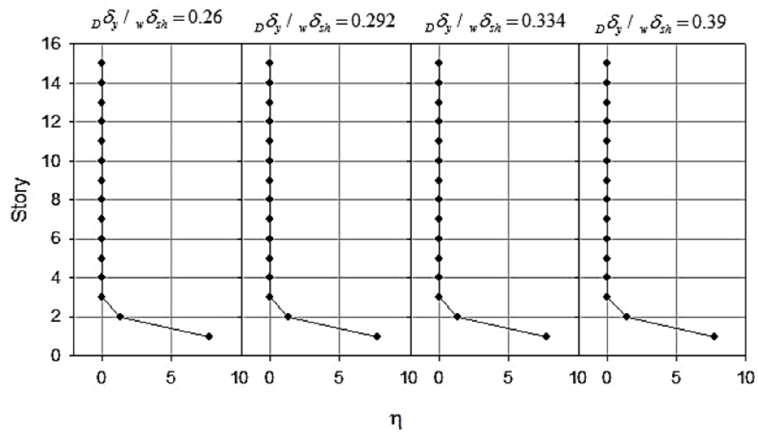

Figure 23. Distribution of cumulative shear plastic deformation of wall piers at different deformation ratio (El Centro NS).

The FSRF is defined as:

$$R_F = 2 - \left(\frac{M_2}{M_1} + \frac{M_3}{M_2} \right) \tag{10}$$

where M_1 is the flexural yield strength of the wall when the wall designed by flexible damper. M_2 is the reduced flexural strength at optimum yield deformation ratio and M_3 is the flexural yield strength at optimum yield deformation

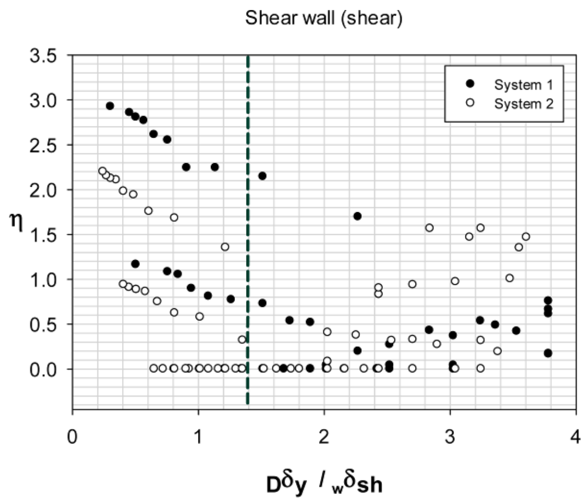

(a) Shear wall at base (shear damage response El Centro NS)

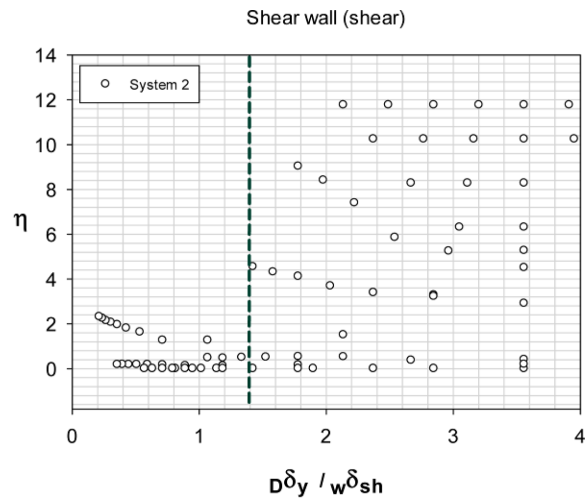

(b) Shear wall at base (shear damage response Hachinohe NS)

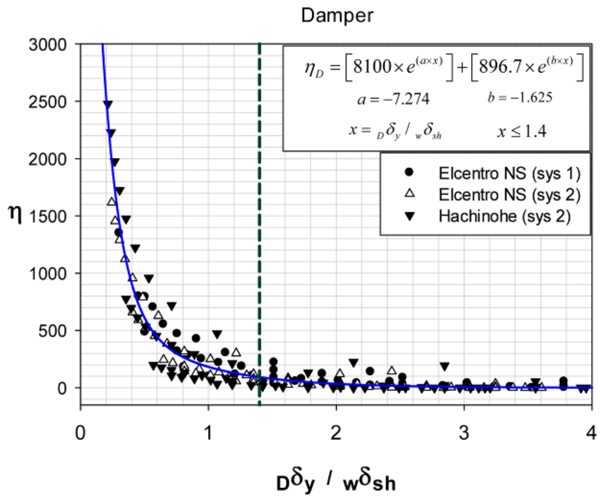

(c) Maximum damage response of dampers

Figure 24. Structural responses due to variation of $_D\delta_y$ (20 Story, T_{sys1} =1.9 sec, T_{sys2} =1.69 sec).

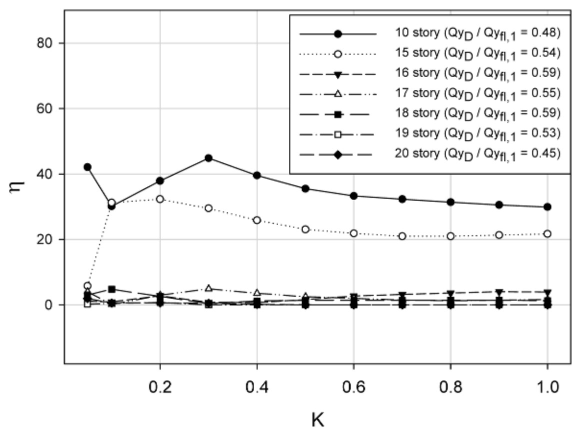

Figure 25. Variation of shear response at the wall base in different height of story buildings (El Centro NS 1940).

ratio considering the target flexural ductility at the wall base.

Figure 26 shows the normalized flexural strength of wall piers that is drawn at the optimum range of deformation ratio. The black line represents the response of flexural strength of the wall using the flexible damper device when the sum of the cumulative shear and flexure of wall at the base is 6 (η=6). The red line represents the reduced flexural strength of wall after using damper that its characteristics are designed based on the optimum yield deformation ratio; whereas the shear damage takes place in the walls. The blue line represents the optimum flexural strength after reduction for walls that damper characteristics selected in the range of the optimum yield deformation ratio for different story buildings considering flexural and shear damage at the accepted level (η=6).

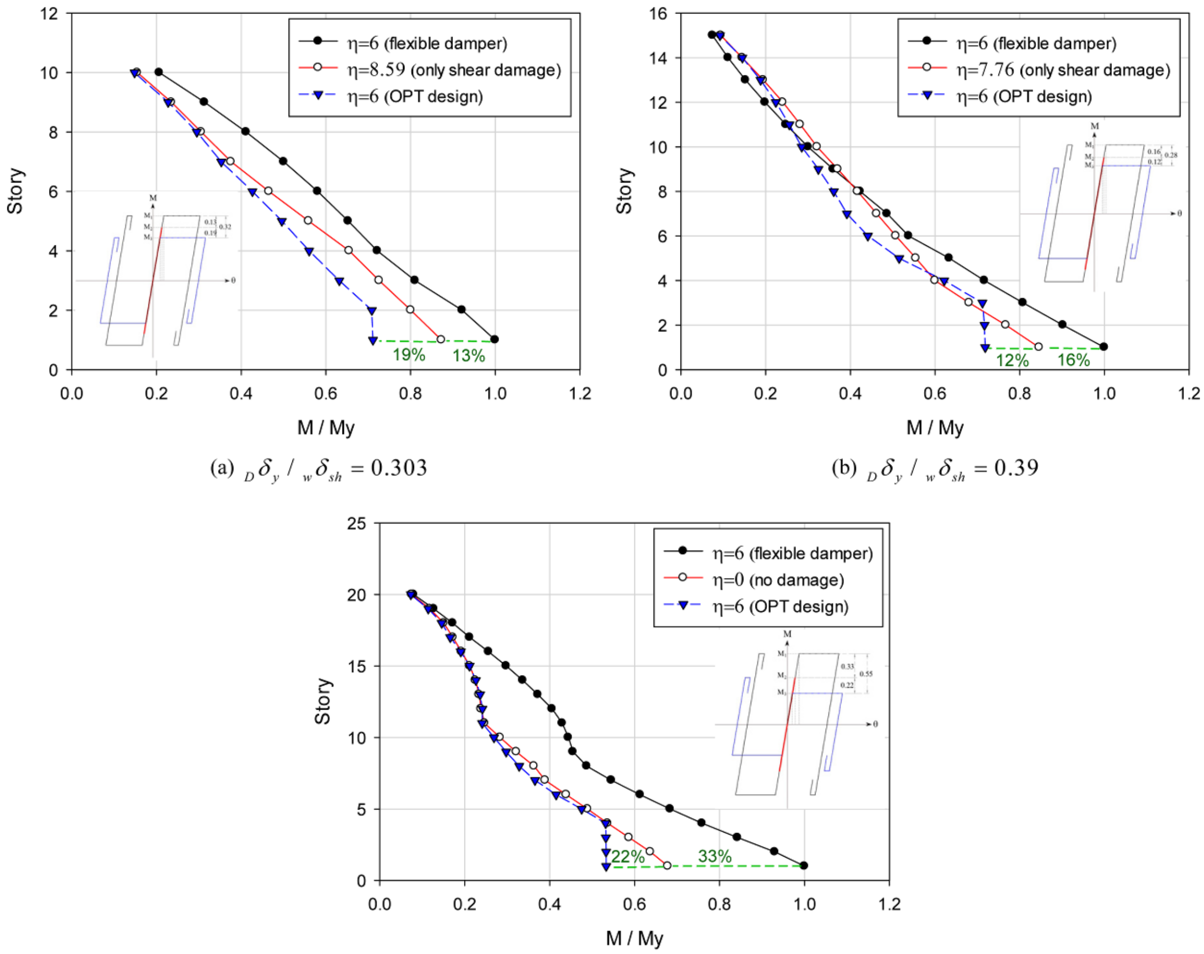

(a) ${}_D\delta_y \,/\, {}_w\delta_{sh} = 0.303$ (b) ${}_D\delta_y \,/\, {}_w\delta_{sh} = 0.39$

(c) ${}_D\delta_y \,/\, {}_w\delta_{sh} = 1.1$

Figure 26. Flexural strength responses of wall piers (El Centro NS 1940).

Table 3. FSRF

Story	T (sec)	M1→M2 (%)	M2→M3 (%)	Total (%)
10 (sys 2)	0.53	13	19	32
15(sys 2)	1.02	16	12	28
20(sys 2)	1.69	33	22	55

Table 3 clearly shows the reduction factor of flexural strength of wall piers for the 10, 15 and 20 story building at any step of the design.

5.4. Shear strength amplification factor (SHSAF) at walls

Shear strength is a function of the flexural ductility; therefore, special care is needed when plastic hinges form in walls. As plastic-hinge rotations increase, the widening of flexure-shear cracks reduces the capacity for shear transfer by aggregate interlock, and the shear strength reduces. However, in some cases, increasing the flexural damage in wall base reduces the shear damage on walls, and thus the amplification factor for shear strength in order to control the shear damage would be reduced.

Table 4. Shear strength enhancement factor

Story	T (sec)	Q1→Q3 (%)
10 (sys 2)	0.53	1
15 (sys 2)	1.02	4
20 (sys 2)	1.69	-16

Increasing the shear capacity of the wall pies by adding the shear reinforcement or increasing the shear size of wall piers may be the effective rehabilitation measures. In this study, the shear strength amplification factor obtained by adding the shear reinforcement. However, as it is shown in Table 4 for 20 story building, after using dampers with the specified stiffness and strength, the shear damage decreased and thus, the shear strength should be decreased about 16% in order to increase the shear damage at the permissible level and not being too conservative.

5.5. Story drift

Figure 27 shows maximum story drift for the system two at each floor of the structures. The maximum story

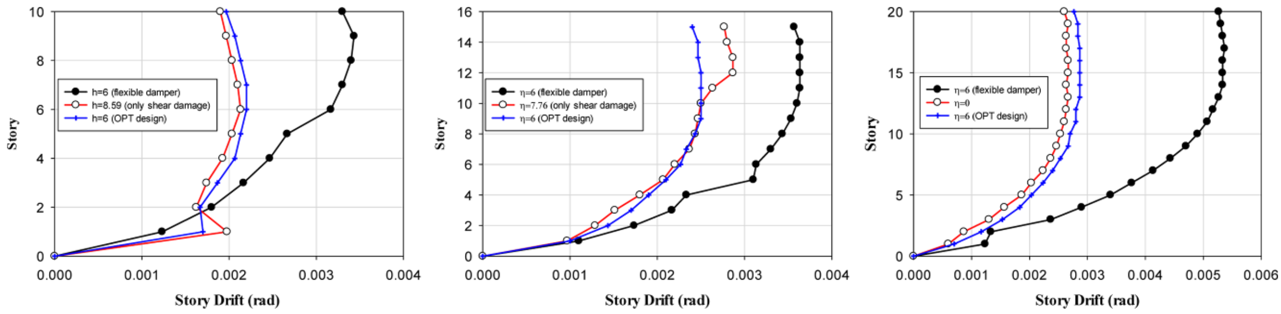

(a) 10 story building (b) 15 story building (c) 20 story building

Figure 27. Maximum story drift at each story (El Centro NS 1940).

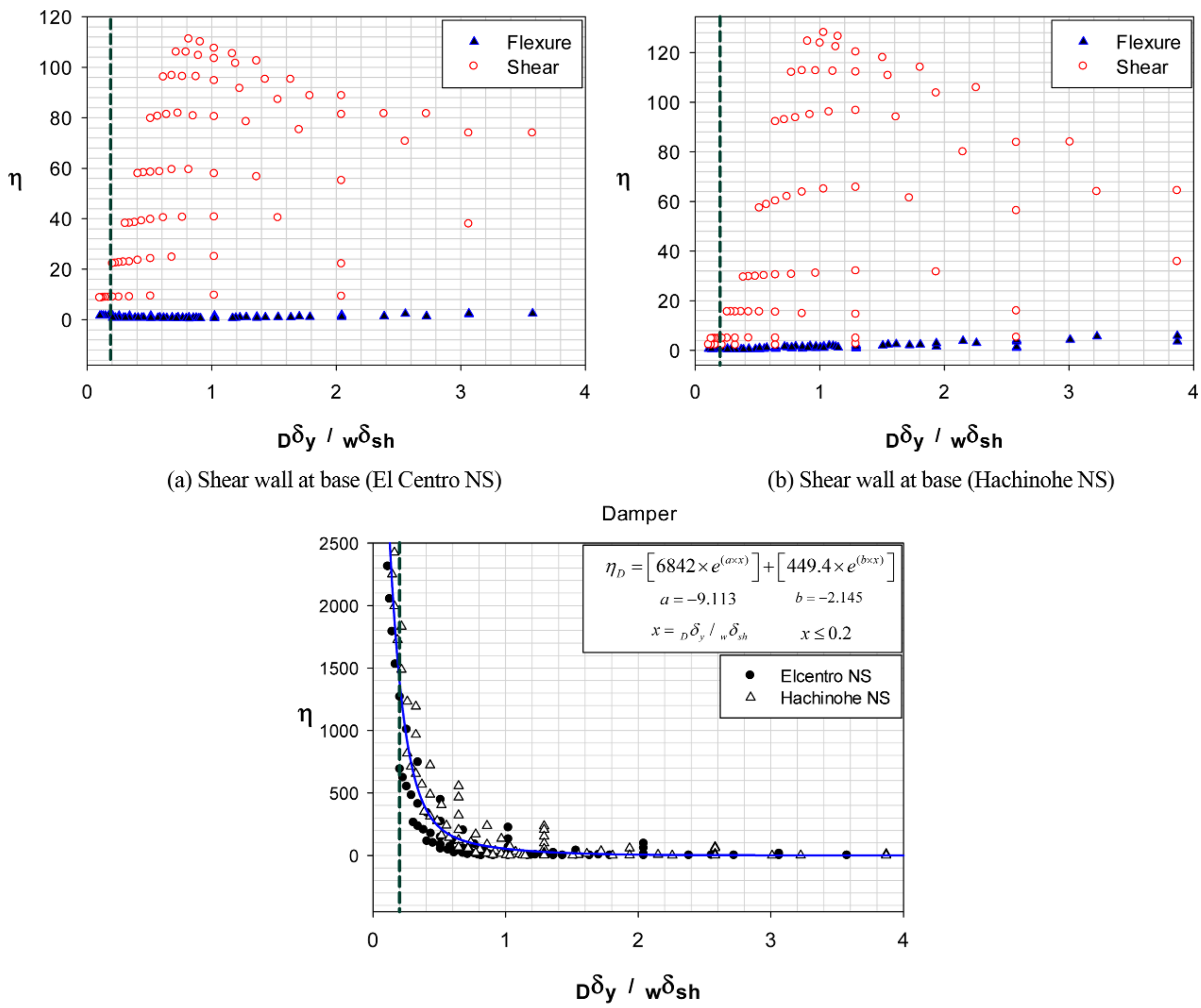

(a) Shear wall at base (El Centro NS) (b) Shear wall at base (Hachinohe NS)

(c) Maximum damage response of dampers

Figure 28. Structural response due to variation of $_D\delta_y$ (10 Story, T=1.04 sec).

drifts of optimum designed system are 1/349, 1/411 and 1/455 for the 10, 15 and 20 story buildings respectively. Compared with the system having flexible dampers with the maximum story drift of 1/291, 1/275 and 1/186, the displacement response is reduced by 16, 33 and 59%.

5.6. Performance of walls at the different range of natural vibration periods:

The previous discussions were for the buildings in the short range natural vibration period. In order to demonstrate the different behavior of buildings in the different natural

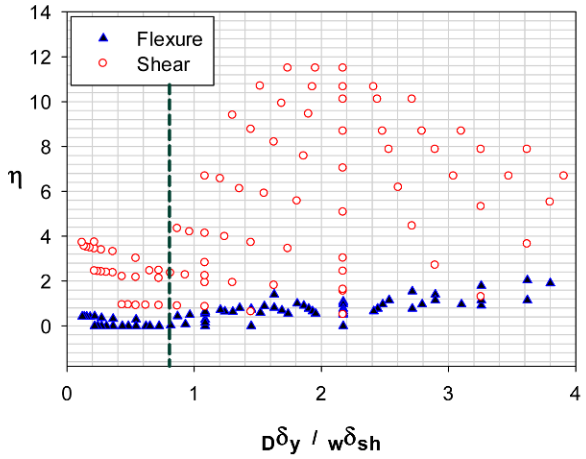

(a) Shear wall at base (El Centro NS)

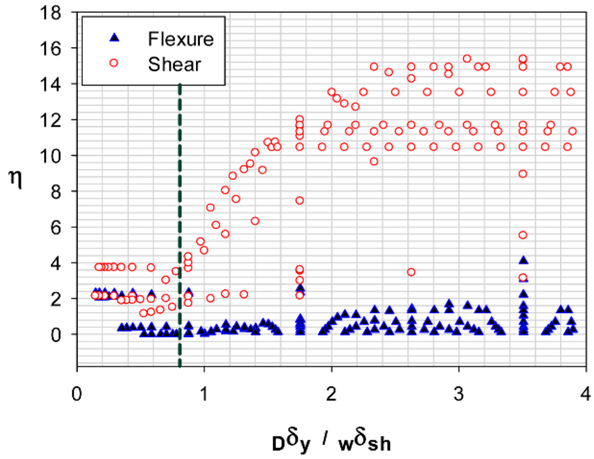

(b) Shear wall at base (Hachinohe NS)

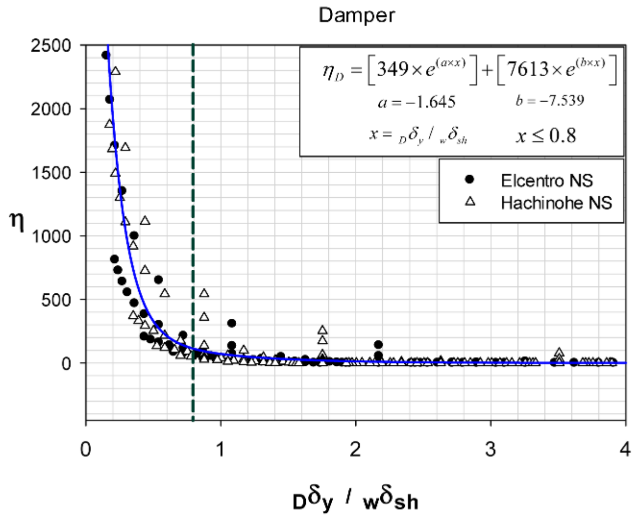

(c) Maximum damage response of dampers

Figure 29. Structural response due to variation of ${}_D\delta_y$ (15 Story, T=2.01 sec).

vibration periods, the results of 10, 15 and 20 story buildings of system 2 discussed here. In this section, plotting Figures similar to the Figs. 12-18 were skipped due to their multiplicity but their descriptions are as follows.

The results prove that by increasing the natural vibration period of the structures, unlike the buildings with the shorter natural time period, the flexural damages at wall appear and the shear damage would be increased by increasing the stiffness ratio of wall-damper.

At the lower yield strength ratio the cumulative shear plastic deformation will be decreased. By increasing the stiffness of the dampers, at the lower yield strength ratio, the shear and flexural damage will be decreased insignificantly. But at the higher yield strength ratio, the shear damage increase significantly and the flexural damage decreases slightly.

The optimum ranges of deformation ratio are selected in order to have less flexure and shear damage at the wall bases. It is obviously showing that the shear and flexural response of wall piers would be better controlled with a lower deformation ratio in a certain range. However, by selecting the optimum range of deformation ratio, the shear strength of wall piers still need to be increased either by adding shear reinforcement or increasing the shear size of the walls.

As shown in Figs. 28(b), 29(b) and 31(b) which illustrate the result of flexural at wall base for 10, 15 and 20 story building respectively, although there is a flexural damage at wall piers, it's still less compare to the structure which designed by flexible damper at the optimum deformation ratio. However Figs. 30(b) and 32(b) prove that by increasing the time period of the structure, the flexural damage would increase significantly and must be taken into consideration.

5.6.1. Flexural strength reduction and shear strength amplification factor

In order for obtaining the reduction and amplification

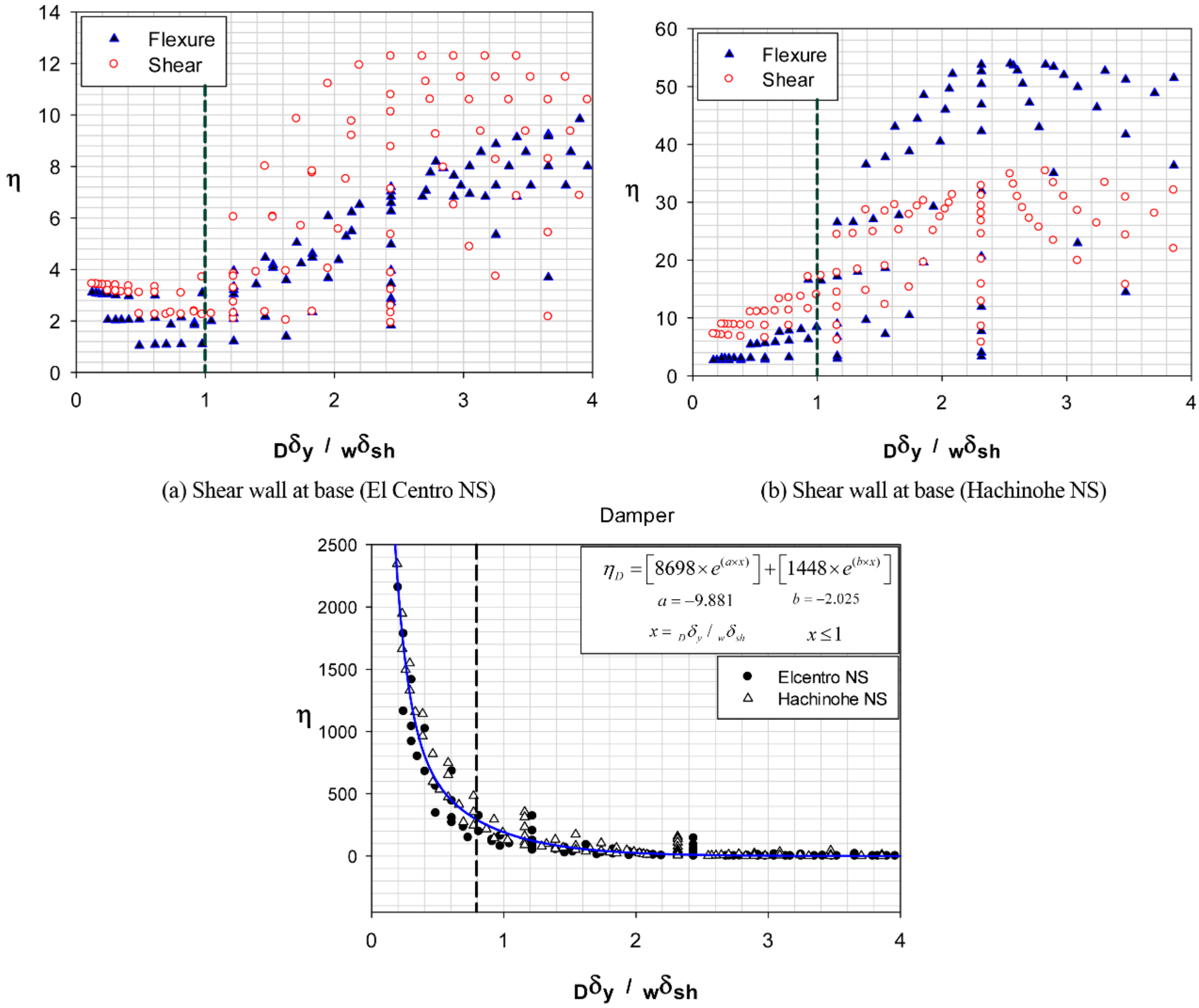

(a) Shear wall at base (El Centro NS)

(b) Shear wall at base (Hachinohe NS)

(c) Maximum damage response of dampers

Figure 30. Structural response due to variation of $_D\delta_y$ (15 Story, T=2.5 sec).

factor for longer time periods, the factors computed according to the Table 3 and 4 For the 10, 15 and 20 story coupled shear wall buildings. Appearing the flexural damage at the wall base, the amount of flexural strength M_2 exceeds the M_1 in all cases; means there will be no reduction at this stage. But still the amount of flexural damage is below the damage considered in the prior design concept, except the 20 story building with having time period of 3.3 Sec. Therefore, in order to consider the permissible flexural damage at wall base, the flexural strength should be reduced. However, Table 5 illustrates that the percentage of flexural strength reduction factor is -10 in the case of 20 story building in the time period of 3.3 Sec, it means unlike the structure in shorter natural period, the flexural strength need to be enhanced in order to minimize the flexural damage at wall base. In addition, in 15 story building at the time period of 2.5 Sec, there is no reduction in flexural strength, because the damage is in permissible level of the design. The shear strength amplification factor at Table 6 computed similar to the Table 4.

5.7. Optimum range of deformation ratio

It has been proven that, if the ratio of the yield deformation of energy dissipation device and deformation at the middle portion of the beam in the first story induced by the flexural behavior of shear walls ($_D\delta_y/_w\delta_{sh}$) is in the below of specific value, the most damage is concentrated on the energy dissipation devices and the walls would have less shear and flexure damage at the base. The optimum ranges of deformation ratio for the different story buildings by having different natural vibration periods are found so as to satisfy selection of energy dissipation device's characteristics. As illustrated in Fig. 33, the maximum range of optimum deformation selected as 0.2, 0.4 and 1.0 for the 10, 15 and 20 story buildings respectively. In order to find the optimum value for the buildings below 20 floors, either using the Eq. 11 which obtains from Fig. 34 or the interpolation method is suggested. Furthermore, for the structures higher than a

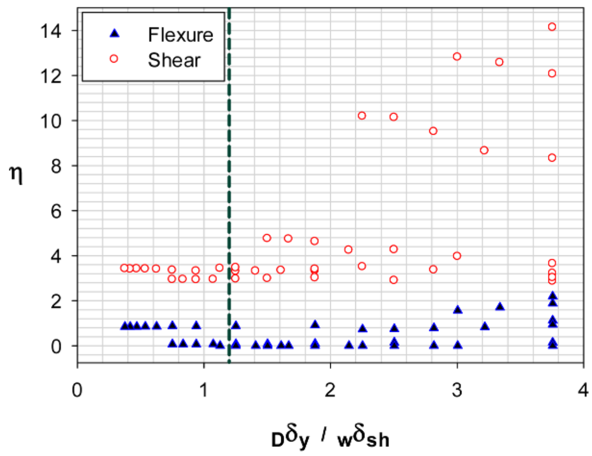

(a) Shear wall at base (El Centro NS)

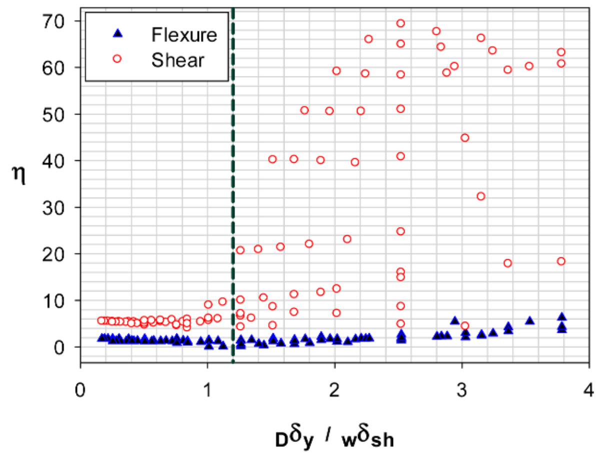

(b) Shear wall at base (Hachinohe NS)

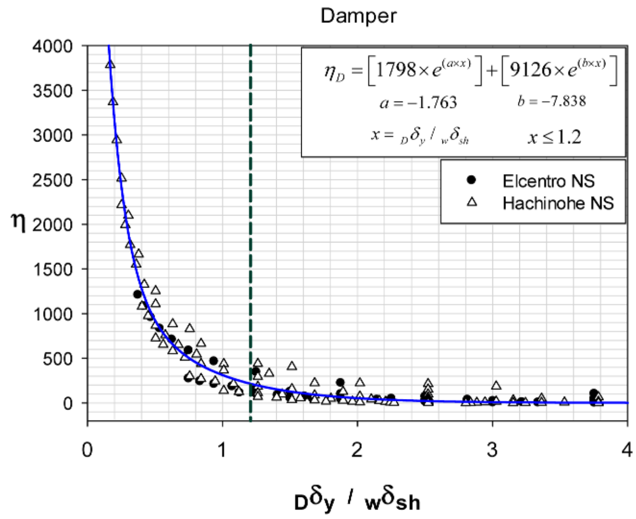

(c) Maximum damage response of dampers

Figure 31. Structural response due to variation of $_D\delta_y$ (20 Story, T=2.5 sec).

20 story building, the same value of 20 story building is suggested.

$$\begin{cases} N \le 20 \quad {}_D\delta_y / {}_w\delta_{sh} = 0.007N^2 - 0.1298N + 0.8126 \\ N > 20 \quad {}_D\delta_y / {}_w\delta_{sh} = 1 \end{cases} \tag{11}$$

where N is the number of stories.

5.8. Effect of damper on the time period of structures

Figure 35 shows that how the stiffness of dampers affects the natural period of vibration. Modal analysis shows that dampers only remarkably affect the first order of systems' natural period; the first period reduces as stiffness ratio K increases. In order to show the effect of stiffness ratio on the high modes of vibration, Fig. 36 demonstrates the result of three orders of the period of vibration in 10, 15 and 20 story buildings.

6. Optimum Distribution of Yield Shear Force Coefficients of Dampers

The optimum distribution of yield shear force coefficients is to evenly distribute the damage over the structural height based on the cumulative plastic deformation ratio of each story. The optimum distribution for the pure shear system and the flexure shear system has been proposed by Akiyama (1985). He suggested the calculation formula for the multi-mass system model with the restoring force characteristic of elastic-perfectly plastic in which the mass distribution of each story is equalized. The optimum distribution of yield shear force coefficients of the pure shear system is:

For $0.2 < x_i \le 1.0$

$$\bar{\alpha}_i = 1 + 1.5927x_i - 11.852x_i^2 + 42.583x_i^3 - 59.48x_i^4 + 30.16x_i^5 \tag{11}$$

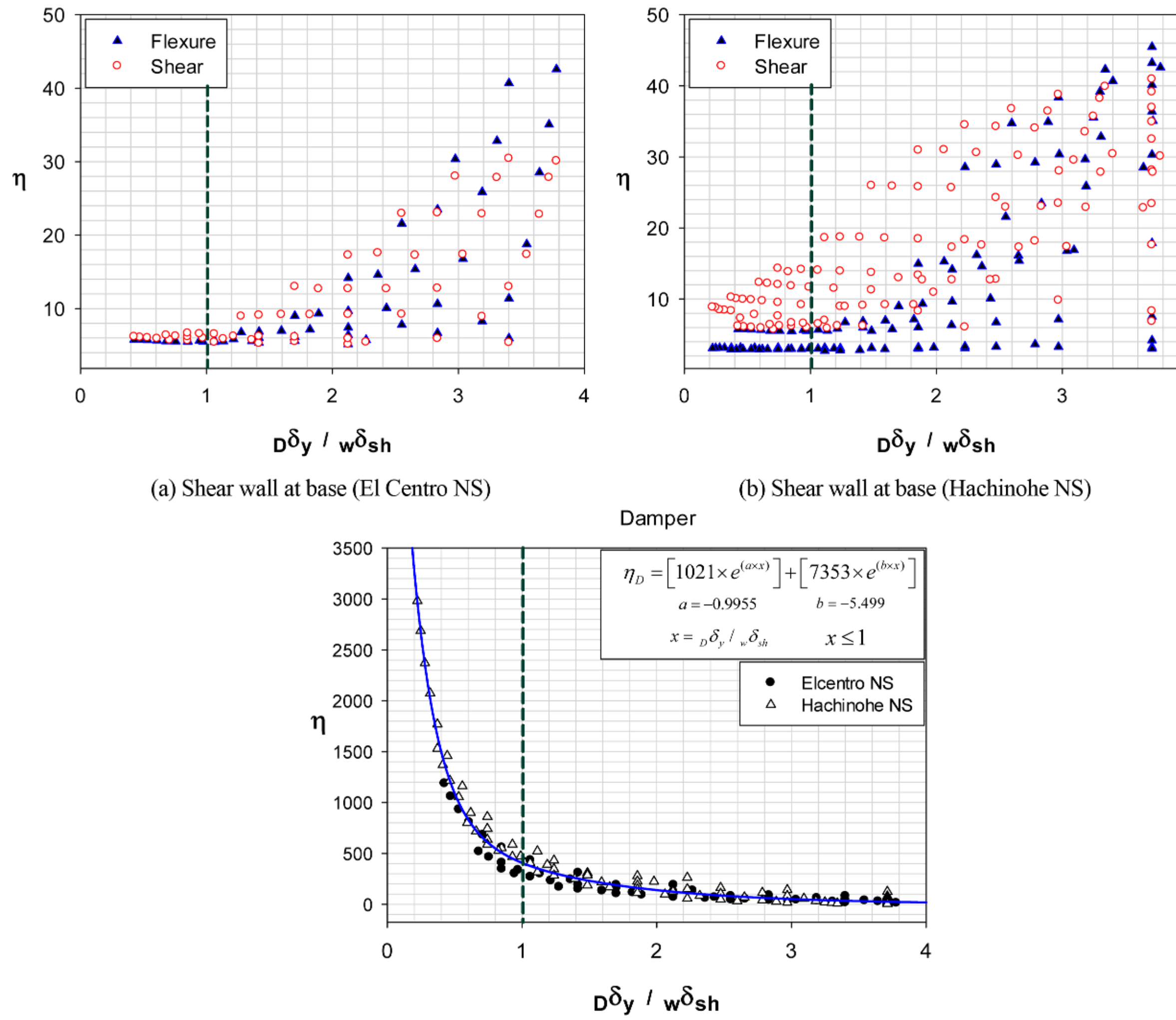

(a) Shear wall at base (El Centro NS)

(b) Shear wall at base (Hachinohe NS)

(c) Maximum damage response of dampers

Figure 32. Structural response due to variation of $_D\delta_y$ (20 Story, T=3.3 sec).

Table 5. FSRF

Story	T (sec)	M1→M2 (%)	M2→M3 (%)	Total (%)
10	1.04	0	9	9
15	2	0	18	18
	2.5	0	0	0
20	2.5	0	13	13
	3.3	0	-10	-10

Table 6. Shear strength amplification factor

Story	T (sec)	Q1→Q3 (%)
10	1.04	10
15	2	3
	2.5	3
20	2.5	1
	3.3	9

For $x_i \le 0.2$ $\quad \overline{\alpha}_i = 1 + 0.5 x_i$

The optimum distribution of yield shear force coefficients in the flexure shear system is:

$$\overline{\alpha}_b = \overline{\alpha}_i + 1.25 x_i^4$$

where: $x_i = (i-1)/N$ (i is the considered story, N is the number of stories), $\alpha_i = Q_{yi} / \sum_{j=i}^{N} m_j g$ (α_i is the yield shear force coefficient of i story).

Instead of the above Equation, a trial and error iterative procedure could be used to find more refined strength distribution from dynamic analysis in order to have an evenly damage through the height of the building (Benavent-Climent *et al.*, 2011; Bagheri *et al.,* 2016).

Oh *et al.* (2014) studied on the optimum distribution of story shear force coefficients in order to improve the seismic performance by distributing the seismic load evenly on all stories. The characteristics of layer damage

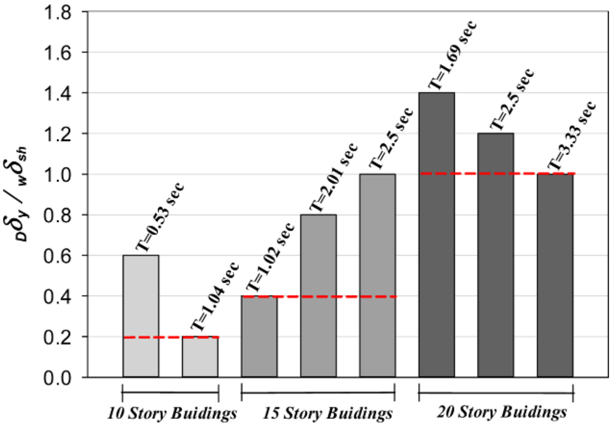

Figure 33. Optimum range of deformation ratio.

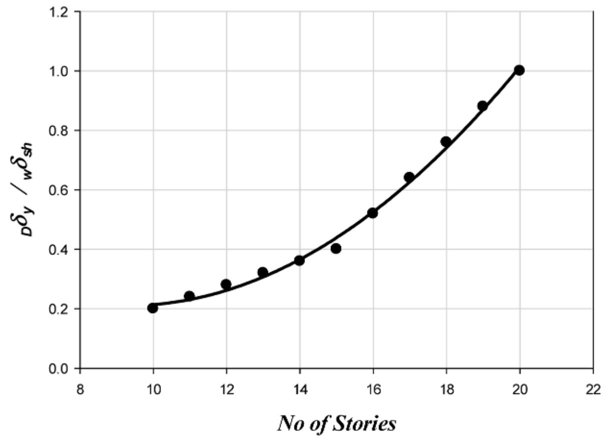

Figure 34. Relation between number of stories and the optimum deformation ratio.

distribution compared based on seismic code of several countries around the world. The seismic efficiency such as layer damage distribution and energy absorbing capacity are analyzed by conducting the response analysis of structures. Thus, they drew the optimum distribution of story shear force in diagrams, which uniformly distributed the layer damage to all stories, and proposed the calculation formula accordingly. The generalized curve of optimum

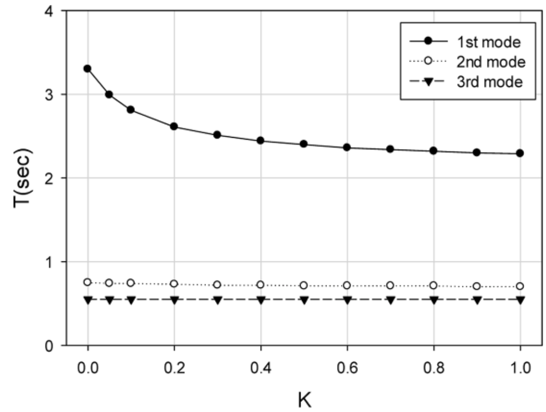

Figure 36. variations of natural periods of vibration due to stiffness ratio K.

distribution of story shear force coefficients considers the variety of natural vibration period of the structure.

$$\bar{\alpha}_i = 1 + \left\{ A \times \left(x_i \right)^B \right\} \tag{12}$$

where, $A = -0.08 \times T^2 + 1.05 \times T + 0.6$, $B = 0.03 \times T^2 + 0.8 \times T + 0.87$ and T is the natural vibration period.

The above proposed equations imply that the yield shear force distribution of the buildings decreases from the bottom to the top floor. However, as discussed in the previous sections, the dampers have shown the different behavior through building's height. Figures 37 and 38 show the behavior of dampers at which the parameters of dampers selected in the optimum range of deformation ratio. The accelerogram used is the El Centro NS 1940 earthquake record. As it is shown in the bar charts, the black bars that indicate the most concentration damages in all cases are from the middle height of the buildings to the top floors which are the maximum amount of damage at dampers. Although there are damages at the lower stories, they are much less compared to the upper stories. The red hatched bars indicate the amount of required damage at dampers which can be gained by decreasing the yield strength of the dampers at the lower part of the building in order to increase the cumulative plastic

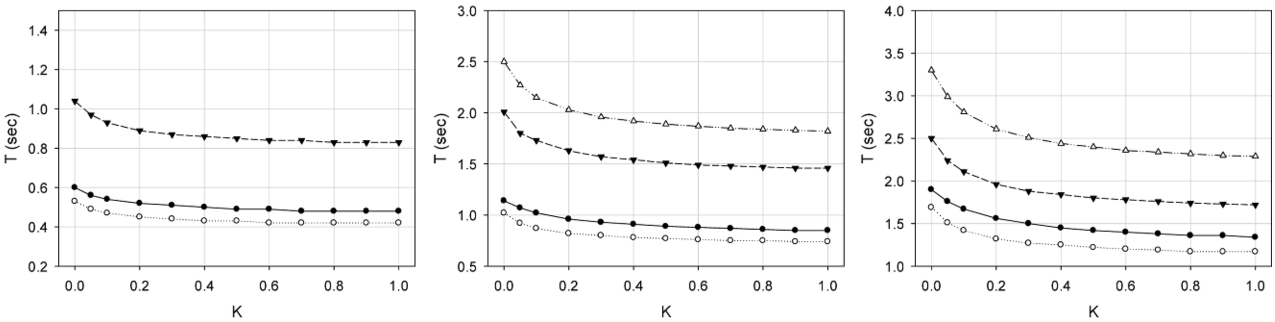

(a) 10 story buildings (b) 15story buildings (c) 20 story buildings

Figure 35. Variation of time period of the structures.

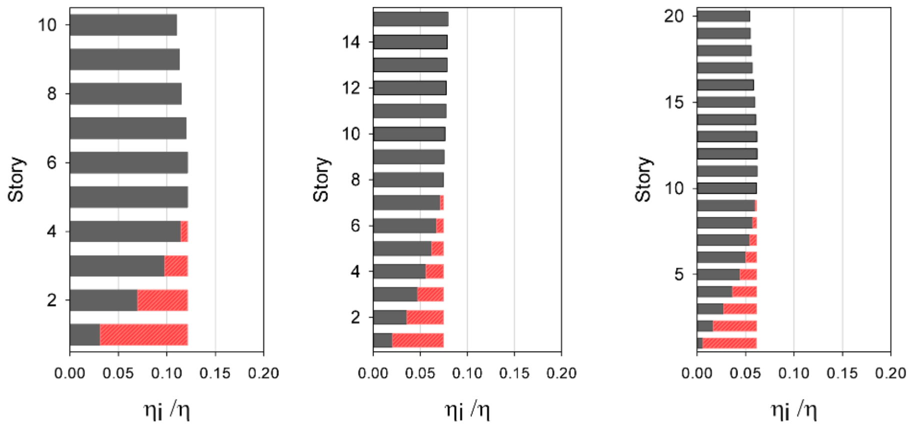

(a) 10 story building (T= 0.53 sec) (b) 15 story building (T=1.02 sec) (c) 20 story building (T=1.69 sec)

Figure 37. Layer damage distribution of dampers through height.

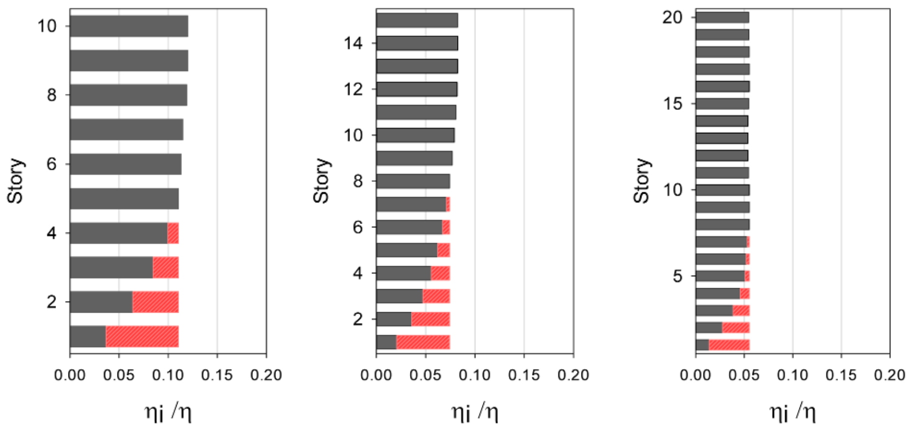

(a) 10 story building (T=1.04 sec) (b) 15 story building (T=2.5 sec) (c) 20 story building (T=3.33 sec)

Figure 38. Layer damage distribution of dampers through height.

deformation ratio up to the amount of damage at upper stories. Therefore, in order to optimize the damage through all stories, evenly distribution of damage at dampers, the new optimum distribution of the yield shear force coefficient of dampers proposed during many dynamic analysis procedures. From the results, it can be concluded that the damage at dampers is nearly equal in the upper part of the shear walls. The generalized curve of the optimum distribution for the different number of story buildings and variety of the natural vibration periods clearly showed a pattern in accordance with the distribution value and the curvature of the curve (The results of optimum distribution of dampers for the 11, 13, 17 and 19 story buildings added to this section). In addition, it showed that the higher the building's height is clearly more likely to show an increasing pattern of the optimum distribution value and the curvature of the graphs in the top portion which related to the dampers at the top portion of the buildings.

The generalized curve of optimum distribution of yield shear force coefficients of dampers follows the shape of an exponential function graph having the minimum value of 1 (Fig. 39). This value is related to the damper at the first floor. Therefore the graph (a) shows the value from bottom to the top of the buildings and the graph (b) shows the value from bottom to the mid-height of the buildings. As it has been mentioned earlier, the damage at dampers in the upper part is nearly equal. Therefore, the strength of dampers at the mentioned part should have the similar value. Since the amount of damage varies on the bottom part, the strength should be changed according to the proposed curve.

In order to clarify the orders of numbers, Fig. 40 illustrates that the building with the even number of stories (for instance 10 story building), the middle height is the middle story and for the building with the odd number of stories (for instance 15 story building), the middle height is the half story upper the middle height of the building.

As stated clearly above, the optimum distribution of yield shear force coefficients of dampers and the number of stories are in overlapped manner and analyzed the pattern accordingly. Thus, the calculation formula of optimum distribution of yield shear force coefficients of dampers described by the variable analysis according to the approximation formula in an exponential model

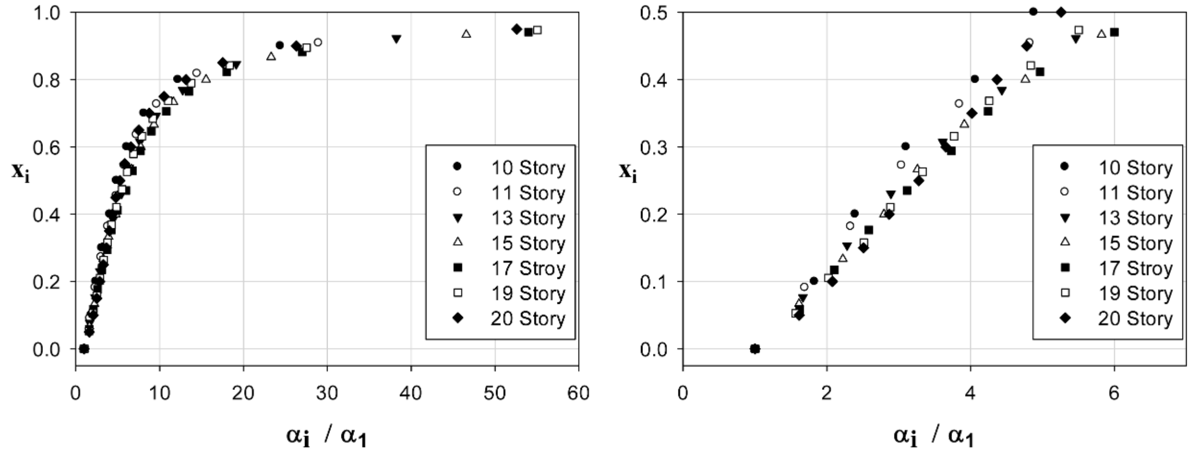

(a) Total height of the building (b) Up to mid-height of the building

Figure 39. Optimum distributions of yield shear force coefficients of dampers ($_D\bar{\alpha}_i = \alpha_i / \alpha_1$).

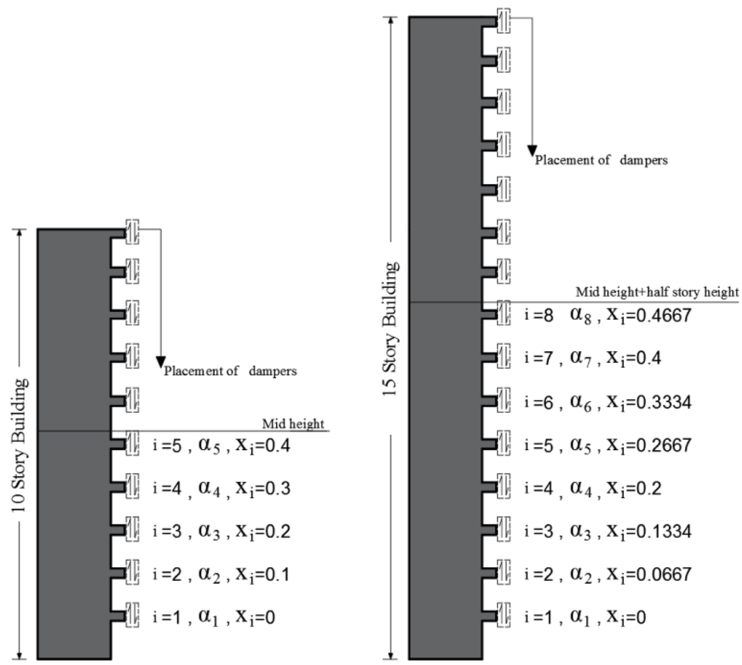

Figure 40. illustration of numbering order.

function form and the number of story buildings is shown in Formula (13). Setting an approximation formula with variables *a*, *b*, *c* and *d*, the variable values for the different number of stories of analytical models are as shown in Fig. 41. The patterns of variables are described in approximation formulas. Figure 42 shows the exactness of the Eq. 13 and the difference with Akiyama's optimum yield-shear force coefficient distribution for the moment resisting frame system obtained by Eq. 11. The vertical line indicates the half of the buildings from bottom to mid-height.

Figure 43 shows the flow chart for the design process of coupled shear wall linked by hysteretic dampers using the energy based design method. In the next section, the flow chart will be clearly elaborate by using examples.

$$\alpha_i / \alpha_1 = 1 + a.\exp(b.x_i) + c.\exp(d.x_i) - (a+c) \quad (13)$$

$$a = 0.0029\exp(-0.6791N) + 6.51E-8 \quad (13\text{-}1)$$

$$b = \begin{cases} 0.678N + 9.98, & 10 \le N < 17 \\ 21.65, & N \ge 17 \end{cases} \quad (13\text{-}2)$$

$$c = 12.07(1-\exp(-0.4589N)) - 10.514 \quad (13\text{-}3)$$

$$d = 624.96(1-\exp(-0.7882N)) - 622.32 \quad (13\text{-}4)$$

where N is the number of total stories.

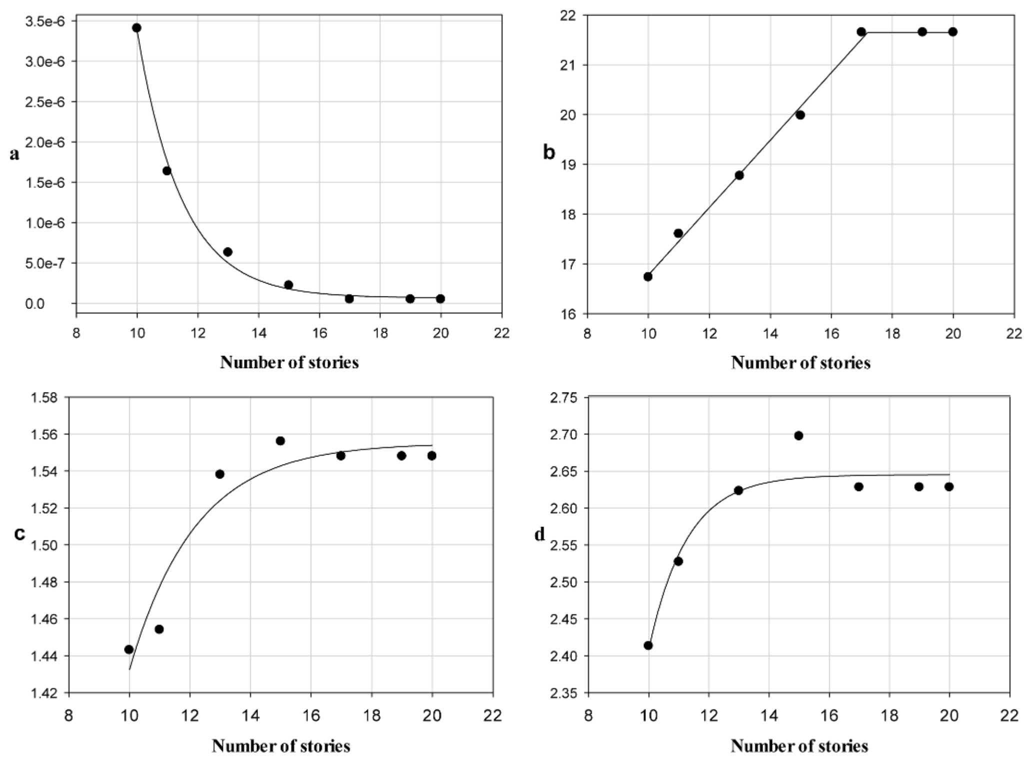

Figure 41. Variable distribution pattern of the proposed approximation formula.

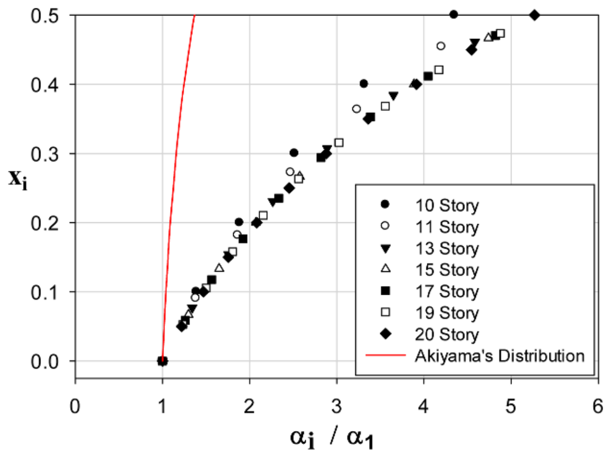

Figure 42. Implementing of Eq. 13 and Akiyama's distribution equation.

7. Numerical Example

Two numerical examples and simulation results are provided to demonstrate the effectiveness and simplicity of the proposed method and the convergence characteristics and numerical stability of the formulation. In the numerical examples, a 15-story building and a 20-story building models with energy dissipation devices placed at the middle portion of coupling beams are used. The properties of the geometry of core walls are provided in Table 7. It is assumed that concrete having a compressive strength of f_c'=21 MPa and a modulus of E =23600 MPa, steel rebar having yield tensile strength of σ_y=350 MPa and a modulus of E =205000 MPa. All the beams in the both models are modeled to behave elastically. Columns are sized based on only gravity load. The stiffness, strength and mass distributions are uniform through the height of buildings. Four accelerograms used in this section. The vibration natural periods are 1.82 Sec and 3.33 Sec for the 15 and 20 story buildings respectively. The damping system considered as 5%. The hysteretic models are the same models as used in this study for the evaluation purpose.

The resulting evaluation criteria are presented for the considered models. The prior design indicates the target damage design at the wall base by having flexible dampers installed at the linked beam in each story (Fig. 44). The target damage value considered as the sum of flexure and shear damages. In this case there will be no damage or absorbing energy by dampers. Hence, all the energy absorption concentrates at the wall and the wall base experience damages.

The next step is to find the optimum characteristics of damper elements according to the proposed optimum deformation ratio in section 5.5. $0 < {}_D\delta_y \,/\, {}_w\delta_{sh} \leq 0.4$ and $0 < {}_D\delta_y \,/\, {}_w\delta_{sh} \leq 1.0$ are the optimum ranges for the 15 and 20 story buildings respectively. In order to find the optimum characteristics of dampers, the trial and error procedure applied. The final trial and error procedure should be considered the less damage at walls (including flexure and shear) and dampers according to the stiffness and strength of dampers. It was proven that selection either the large stiffness of dampers or the low yield

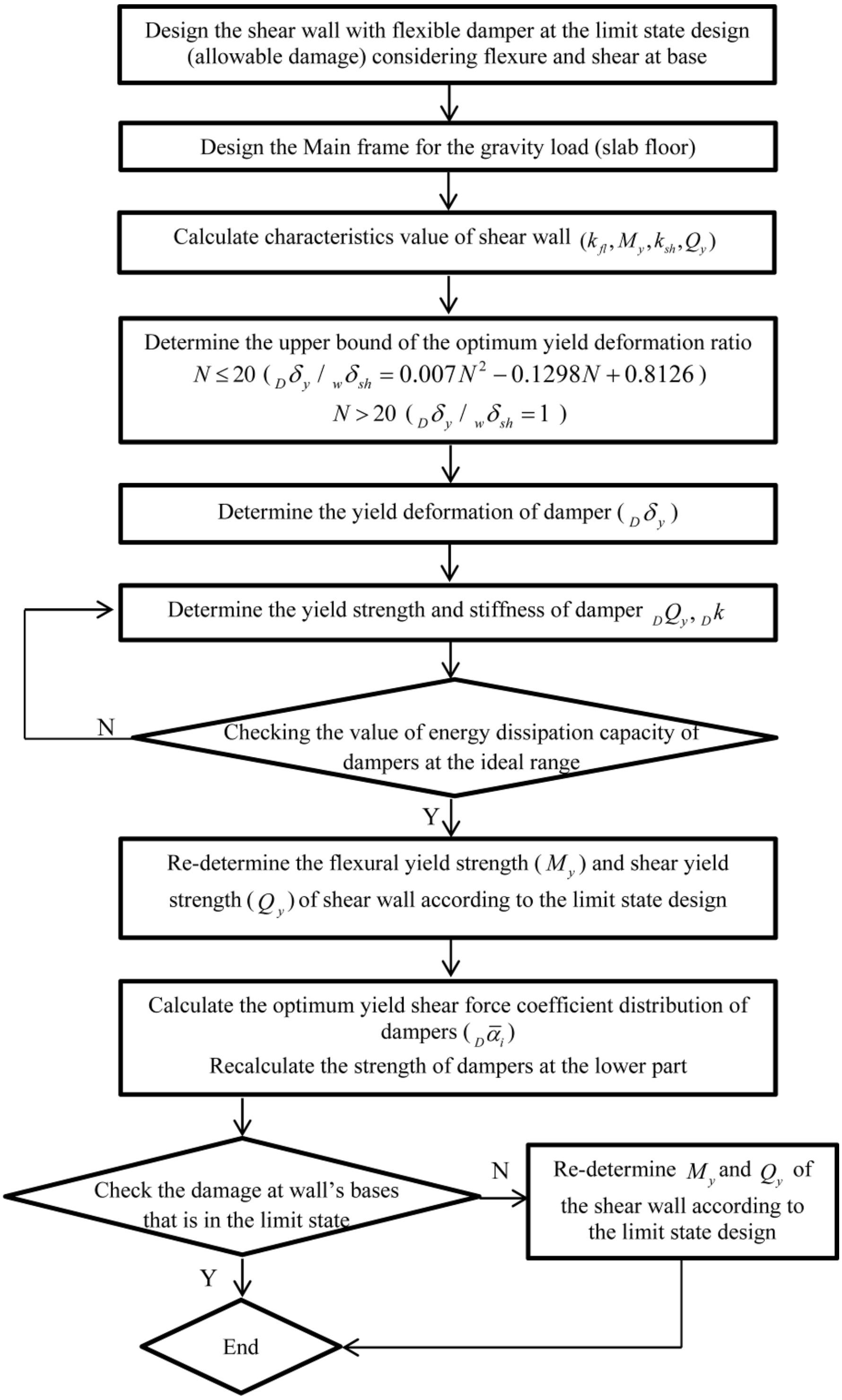

Figure 43. Flowchart of design procedure.

Table 7. Walls section properties

Example	a (m)	b (m)	c (m)	EI (kN·m^2) (Flexural stiffness)	AG/(6/5) (kN·m) (Shear stiffness)	AE (kN) (Axial Stiffness, compression)
Ex1. 15 story Building	6	1	0.45	191228445	22132921.5	63742815
Ex2. 20 story Building	6.5	1	0.45	243130147	23977332	69054716

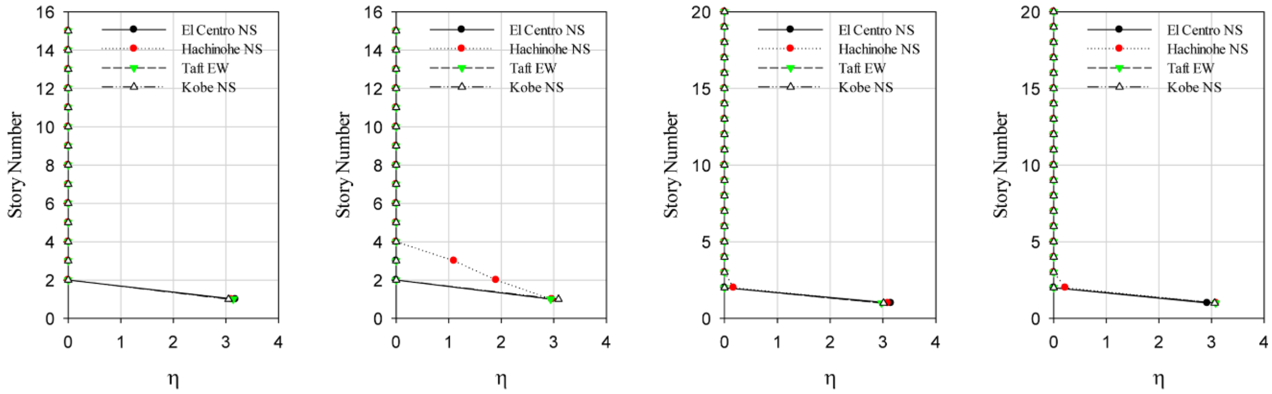

(a) 15 story building in flexure (b) 15 story building in shear (c) 20 story building in flexure (d) 20 story building in shear

Figure 44. Cumulative plastic deformations of walls.

Table 8. Design procedure

Earthquake records	Story Building	Trial 1					Trial 2					Trial 3					Re-determine the strength of walls (flexure and shear)			
		K	${}_D\delta_y/{}_w\delta_{sh}$	$Qy_D/Q_{yfl,1}$	η FL	η SH	K	${}_D\delta_y/{}_w\delta_{sh}$	$Qy_D/Q_{yfl,1}$	η FL	η SH	K	${}_D\delta_y/{}_w\delta_{sh}$	$Qy_D/Q_{yfl,1}$	η FL	η SH	FSRF %	SHSAF %	η FL	η SH
El Centro NS	15	0.7	0.17	0.06	0.11	3.01	0.4	0.29	0.06	0.1	2.76	0.4	0.37	0.08	0	2.37	30	-3	3	3
	20	0.6	0.4	0.1	5.34	4.11	0.5	0.48	0.1	5.34	4.08	0.5	0.62	0.13	5.03	4.21	-8	4	3	3
Hachinohe NS	15	0.7	0.12	0.04	0	0.02	0.4	0.22	0.04	0	0.02	0.4	0.33	0.07	0	0	25	-14	3	3
	20	0.6	0.76	0.195	2.73	14.5	0.5	0.85	0.182	2.52	14	0.5	0.79	0.169	2.52	14	3	13	3	3
Taft EW	15	0.8	0.2	0.08	0.08	5.82	0.6	0.26	0.08	0.08	5.72	0.6	0.39	0.16	0.1	5.7	19	15	3	3
	20	0.6	0.91	0.23	0.61	5.84	0.5	0.82	0.17	0.51	5.35	0.5	0.68	0.14	0.46	5.05	15	5	3	3
Kobe NS	15	0.7	0.14	0.05	3.3	6.1	0.4	0.25	0.05	3.3	5.82	0.4	0.37	0.08	3.3	5.8	-2	7	3	3
	20	0.6	0.18	0.04	5.15	5.8	0.5	0.27	0.05	4.8	5.92	0.5	0.36	0.07	4.2	6	-13	1	3	3

Table 9. Optimum distribution of yield shear force coefficients of dampers

15 Story Building	Story No	1	2	3	4	5	6	7	8	-	-
	$x_i=(i-1)/N$	0	0.0667	0.1334	0.2	0.2667	0.3334	0.4	0.4667	-	-
	${}_D\overline{\alpha}_i$	1	1.3	1.65	2.07	2.57	3.17	3.89	4.74	-	-
20 Story Building	Story No	1	2	3	4	5	6	7	8	9	10
	$x_i=(i-1)/N$	0	0.05	0.1	0.15	0.2	0.25	0.3	0.35	0.4	0.45
	${}_D\overline{\alpha}_i$	1	1.22	1.47	1.76	2.08	2.45	2.88	3.36	3.92	4.55

strength ratio is inappropriate as a dissipation device's parameters. Therefore, in Table 8 at trial 2, the stiffness ratio decreased and the yield strength ratio increased compared to the previous trials. "FL" and "SH" indicate the flexural cumulative plastic deformation and shear cumulative plastic deformation at the wall's base respectively. As indicated in the table, the values of FSRF and SHSAF indicate the percent reduction or amplification in order to design based on target damage. These values provide an initial estimate of force reduction or amplification factors required for well-detailed shear wall considering the level performance objectives.

The results of response analysis show the proposed calculation formula of optimum distribution of yield shear force coefficients of dampers provide a preferable distribution for the coupled shear wall system linked by dampers that undergo even damage over all stories. Table 9 indicates the values obtained for the optimum distribution of the yield shear force coefficient from the Eq. 13. It can be seen from Fig. 45 by conducting the optimum distribution of the yield shear force coefficient of dampers, the cumulative plastic deformation at dampers are almost equal in all stories and prevent concentration damage at upper part. However, it is worth to mention that instead of using the

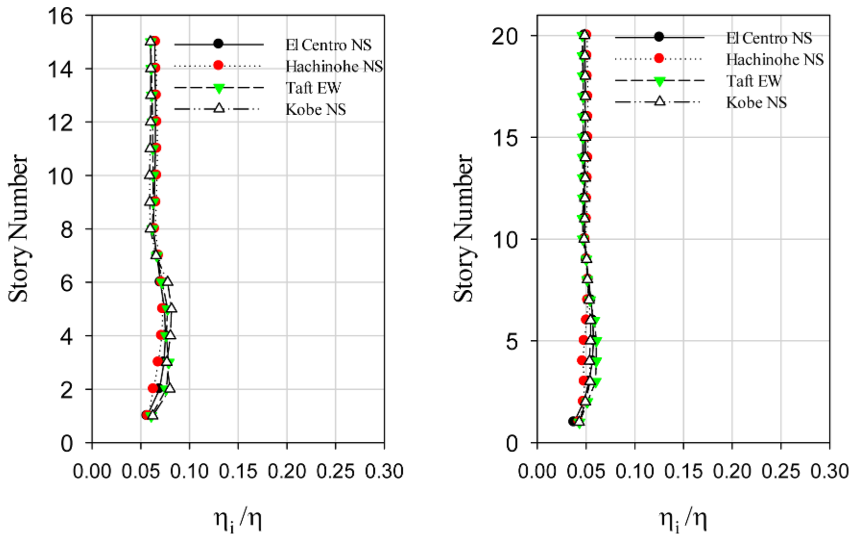

Figure 45. Cumulative shear plastic deformation ratio of dampers through height.

Eq. 13, a trial and error iterative procedure could be used to find more refined strength distribution from dynamic analysis.

8. Conclusions

This paper presents a new philosophy for the design of coupled shear wall buildings where dissipation devices are located in the middle portion of linked beams to introduce a high level of dependable energy dissipation devices for the primary purpose of reducing earthquake effects.

On the basis of the results shown in the previous sections, the following conclusion can be drawn:

(1) Numerical simulation of the different damping wall systems subjected to earthquake is carried out to verify the damping effect of the new structure system. It is also discussed how damper parameters influence the damping wall on the seismic performance, and the discussion presents that only when the parameters are chosen in a certain range would the ideal damping effect be acquired.

(2) The main factors for reduction of the response of the structure are parameters associated with dampers and the dissipation of energy produced during earthquake by the mean of dampers.

(3) The performance of building structures in seismic loading is improved to a great extent. By the provision of optimum designed dampers, maximum drift is reduced by 16, 33 and 59% for 10, 15 and 20 story buildings respectively.

(4) The design procedure adopted for proportioning the coupled shear wall-frame having damper in the middle portion of the coupling beam in shear wall prove to be effective and reliable for controlling the seismic damage of the shear wall.

(5) By using the suitable yield deformation ratio, an appropriate value for the characteristics of dampers can be selected such that the less the damage level of wall and damper is achieved. In order to achieve the accepted damage level at the walls, the flexural and shear strengths of walls need to be changed according to the value of permissible damage.

(6) The results clearly demonstrated that by designing the optimum damper device with the strength reduction factor of and amplification factor of wall piers, greater degree of reliability in the earthquake-resistant design or upgrading of buildings can be achieved.

(7) The damage distribution of dissipation devices applied with the proposed calculation formula of optimum distribution of yield shear force coefficients of dampers showed a relatively uniform distribution through the height of the building.

Acknowledgment

This work was supported by a 2-year Research Grant of Pusan National University.

References

ACI Committee, American Concrete Institute, & International Organization for Standardization. (2008). Building code requirements for structural concrete (ACI 318-08) and commentary. American Concrete Institute.

Akiyama, H. (1985). *Earthquake-resistant limit-state design for buildings*. Univ of Tokyo Pr., Japan.

Bagheri, B., Choi, K.Y., Oh, S.H. and Ryu, H.S., 2016. Shaking table test for evaluating the seismic response characteristics of concentrically braced steel structure with and without hysteretic dampers. *International Journal of Steel Structures,* 16(1), pp. 23-39.

Benavent-Climent A, Pujades LG, López-Almansa F. Design energy input spectra for moderate-seismicity regions.

Earthquake engineering & structural dynamics. 2002 May 1, 31(5), pp. 1151-1172.

Benavent-Climent, A. (2011). An energy-based method for seismic retrofit of existing frames using hysteretic dampers. *Soil Dynamics and Earthquake Engineering*, *31*(10), pp. 1385-1396.

Bertero, V. V. (1980). Seismic Behaviour of RC Wall Structural Systems. In *Proceedings of the 7th WCEE*.

Chung, H. S., Moon, B. W., Lee, S. K., Park, J. H., & Min, K. W. (2009). Seismic performance of friction dampers using flexure of RC shear wall system. *The Structural Design of Tall and Special Buildings*, *18*(7), pp. 807-822.

Harries, K. A., Gong, B. and Shahrooz, B. M. (2000), "Behavior and Design of Reinforced Concrete, Steel, and Steel-Concrete Coupling Beams," *Earthquake Spectra,* 16(4), pp. 775-799.

Harries, K. A., Shahrooz, B. M., Brienen, P., Fortney, P. J., & Rassati, G. A. (2006). Performance-Based Design of Coupled Wall Systems. In *Composite Construction in Steel and Concrete V*, pp. 686-697.

Housner, G. W. (1956). Limit design of structures to resist earthquakes. In *Proc. of 1st WCEE*, pp. 5-1.

Kim, H. J., Choi, K. S., Oh, S. H., & Kang, C. H. (2012). Dissipative Coupling Beams used for RC Shear Walls Systems. *15WCEE, Lisboa, Portugal, September*.

Kurama, Y. C., & Shen, Q. (2004). Posttensioned hybrid coupled walls under lateral loads. *Journal of Structural Engineering*, 130(2), pp. 297-309.

Lefas, I. D., & Kotsovos, M. D. (1990). NLFE analysis of RC structural walls and design implications. *Journal of Structural Engineering*, 116(1), pp. 146-164.

Lequesne, R., Setkit, M., Kopczynski, C., Ferzli, J., Cheng, M. Y., Parra-Montesinos, G., & Wight, J. K. (2011). Implementation of High-Performance Fiber Reinforced Concrete Coupling Beams in High-Rise Core-Wall Structures. *American Concrete Institute, ACI, Special Publication*, 280, pp. 1-12.

Madsen, L. P. B., Thambiratnam, D. P., & Perera, N. J. (2003). Seismic response of building structures with dampers in shear walls. *Computers & structures*, 81(4), pp. 239-253.

Naish, D., Wallace, J. W., Fry, J. A., & Klemencic, R. (2009). Reinforced concrete link beams: Alternative details for improved construction. *UCLA-SGEL Report*, 6, pp. 1-103.

Oh, S. H., Choi, K. Y., Kim, H. J., & Kang, C. H. (2012). Experimental validation on dynamic response of RC shear wall systems coupled with hybrid energy dissipative devices. *15WCEE, Lisbon, Portugal, Paper-ID*, 1422, pp. 24-28.

Oh, S. H., & Jeon, J. S. (2014). A study on optimum distribution of story shear force coefficient for seismic design of multi-story structure. *International Journal of High-Rise Building*, 2, pp. 121-145.

Parra-Montesinos, G. J. (2005). High-performance fiber-reinforced cement composites: an alternative for seismic design of structures. *ACI Structural Journal*, 102(5), pp. 668.

Paulay, T., & Binney, J. R. (1974). Diagonally reinforced coupling beams of shear walls. *Special Publication*, 42, pp. 579-598.

Paulay, T., & Santhakumar, A. R. (1976). Ductile behavior of coupled shear walls. *Journal of the Structural Division*, 102(1), pp. 93-108.

Paulay, T., & Priestley, M. N. (1992). *Seismic design of reinforced concrete and masonry buildings*.

Priestley, M. J. N., Calvi, G. M., & Kowalsky, M. J. (2007). Direct displacement-based seismic design of structures. In *2007 NZSEE conference*.

Rosmon, R. (1964, June). Approximate analysis of shear walls subject to lateral loads. In *Journal Proceedings* 61(6), pp. 717-734.

Smith, B. S., Coull, A., & Stafford-Smith, B. S. (1991). *Tall building structures: analysis and design* (Vol. 5). New York: Wiley.

Subedi, N. K. (1991). RC-coupled shear wall structures. I: Analysis of coupling beams. *Journal of Structural Engineering*, 117(3), pp. 667-680.

Sullivan, T. J., & Lago, A. (2010). Retrofit of RC wall buildings using viscous dampers. In *14th European Conference on Earthquake Engineering*.

Vecchio, F. J. (1992). Finite element modeling of concrete expansion and confinement. *Journal of Structural Engineering*, 118(9), pp. 2390-2406.

Zahrah, T. F., & Hall, W. J. (1984). Earthquake energy absorption in SDOF structures. *Journal of structural Engineering*, 110(8), pp. 1757-1772.